Fabrication of Thymine Immobilized Magnetic Graphene Oxide for The Efficient Removal of Mercury and Melamine

by

ABDULLA-AL-MAMUN
STUDENT ID: 0417032706

MASTER OF SCIENCE IN CHEMISTRY

Department of Chemistry
BANGLADESH UNIVERSITY OF ENGINEERING AND TECHNOLOGY
2018

The thesis titled "Fabrication of Thymine Immobilized Magnetic Graphene Oxide for The Efficient Removal of Mercury and Melamine" submitted by Abdulla-Al-Mamun, Roll No.:0417032706, Session: April 2017, has been accepted as satisfactory in partial fulfillment of the requirement for the degree of Master of Science on. 17 October 2018

BOARD OF EXAMINERS

1. Dr. Md. Shafiul Azam
   Assistant Professor
   Department of Chemistry,
   BUET, Dhaka

   Chairman

2. Dr. Md. Abdur Rashid.
   Professor & Head
   Department of Chemistry
   BUET, Dhaka

   Member
   (Ex-officio)

3. Dr. Md. Shakhawat Hossain Firoz
   Professor
   Department of Chemistry
   BUET, Dhaka

   Member

4. Dr. Md. Anamul Haque
   Professor
   Department of Chemistry
   Jahangirnagar University,savar
   Dhaka

   Member
   (External)

CANDIDATE'S DECLARATION

It is hereby declared that this thesis or any part of it has not been submitted elsewhere for the award of any degree or diploma.

Abdulla-Al-Mamun

I dedicate this thesis to.....

My Beloved Mother
&
Honorable Supervisor

List of Tables and Figures

Figures

Tables

List of Abbreviations of Technical Symbols and Terms

1. Graphene oxide (GO)
2. 1-Trimethoxysilylundecylthymine (1-TMSU-T)
3. Magnetic thymine (MT)
4. Magnetic thymine with graphene oxide (MTGO))
5. Thymine immobilized magnetic graphene oxide (MGOT)
6. Thymine immobilized graphene oxide functionalized magnetic thymine (MTGOT)

Acknowledgement

At the beginning, all praises to the almighty Allah who has been given me the strength and opportunity to complete this thesis work as an M.Sc. student the Department of Chemistry at Bangladesh University of Engineering and technology (BUET), Dhaka Bangladesh.

Regarding the outcome of this thesis, The Author expresses his deepest sense of gratitude and respect to his supervisor Dr. Md. Shafiul Azam, Assistant Professor, Department of Chemistry, Bangladesh University of Engineering and Technology for the Scholastic supervision during this research Work.

It is my great honor to convey my sincere gratitude to my respected teacher Professor Dr. Md. Abdur Rashid, honorable Head of the Department of Chemistry, BUET for giving me his wonderful support to move through the academic processes during this M.Sc. program. I would like to convey my deepest gratitude to Professor, Dr. Md. Shakhawat Hossain Firoz, Associate Professor Dr. Abu Bin Imran, Assistant Professor Dr. Chanchal Kumar Roy and Dr. Ayesha Sharmin, Lecturer Nahida Akter Department of Chemistry, BUET, for their valuable suggestions, appreciated comments, guidance and help during the research period.

I am thankful to all other respected teachers of the Department of Chemistry, BUET, for their time to time support. I would also like to thank all of the officers and staffs of the Department of Chemistry, BUET for their continuous help during my study period.

I am highly thankful to Professor Dr. Hongbo Zeng, University of Alberta, Canada for the characterization of our samples using X-ray Photoelectron Spectroscopy (XPS) technique during my research.

I am highly grateful to all members of the board of examiners for their valuable suggestions and appreciated comments.

I would like to express my sincere gratitude to A. K. M. Atique Ullah, Scientific Officer Chemistry Division, Atomic Energy Centre, Bangladesh Atomic Energy Commission, Dhaka, Bangladesh for his generous help and kind support of materials characterization during the research period.

I am thankful to my dear colleagues and all the members of Azam Research Group for their friendly cooperation and lovely encouragement throughout my research period. Special thanks to Md. Majharul Islam and Mohammad Motiur Rahman Imon Md. Ferdous & Bushra Parvin for their continuous help during the research.

I am also thankful to other fellows of Chemistry Materials Laboratory for their cooperation during the research period.

I am grateful to the authority of BUET and The World Academy of Sciences (TWAS) for providing financial support for this research work.

Finally, I would like to express my heartfelt indebtedness and profound gratitude to my beloved father, mother and all of my family members for their continuous inspiration and immeasurable sacrifices throughout the period of my study.

October, 2018 Abdulla-Al-Mamun

Abstract

The presence of harmful inorganic pollutant mercury (Hg^{2+}) and organic contaminant melamine in wastewater causes serious environmental and health problems. Various methods or techniques have been applied for the removal of melamine and mercury from wastewater. Among those methods, the adsorption method has received much attention due to its high efficiency, simplicity and economic validity. In this study, we exploited the strong selective interaction of mercury and melamine with thymine to develop a composite material for the adsorption of these contaminants. Specifically, magnetic graphene oxide was modified by a thymine derivative, 1-trimethoxysilyleundecyle-thymine (1-TMSU-T), to introduce higher Hg (II) and melamine adsorption capacity. The fabrication of thymine-modified magnetic graphene oxide was carried out in two procedures for comparison. In the first procedure, magnetic nanoparticles (Fe_3O_4) were initially coated with thymine and then hydrothermally treated with GO before another thymine modification (hereafter denoted as MTGOT). In another procedure, magnetic graphene oxide (MGO) was directly treated with (1-TMSU-T) in one step to introduce the thymine molecules on the surface (hereafter denoted as MGOT). The fabricated nanomaterials were characterized employing FTIR, XPS, FESEM, EDX and magnetization. The magnetization (magnetization vs magnetic field) hysteresis of the nanomaterials confirmed the magnetic nature of the synthesized materials. Remarkably, these materials exhibit excellent melamine removal performance and high Hg^{2+} adsorption capacities which reveled in different adsorption tests of melamine and Hg^{2+}. MTGOT and MGOT had a Hg^{2+} adsorption capacity of 16.1 mg g^{-1} and 12.4 mg g^{-1}, respectively. It was found that MTGOT and MGOT could remove 94.5% and 77.4%, respectively, of a 20 mL 50 ppm solution.

CHAPTER 3 Results and Discussion

CHAPTER 1

Introduction

1.1. General Remarks

Melamine, a triazine heterocyclic organic compound, has been widely used in the production of plastics, coatings, flame retardants, melamine resins and other products [1]. In the past years, melamine has been illegally and unethically added to the food and animal feeds. On the other hand, mercury is a highly toxic and widespread pollutant that comes from divers' sources including nature and human activities [2]. Both melamine and mercury have toxic effects in human and animal body. The intake of melamine for human and animal could lead to the formation of insoluble complex in kidney and subsequent tissue injury [3]. On the other hand, Mercury (Hg^{2+}) can damage the brain, kidneys, and endocrine system, resulting in often server effect [4]. So, economically viable techniques to efficiently remove mercury and melamine from wastewater are highly desirable. Numerous materials have been developed and investigated including silica [5], hydrogels [6], magnetic beds [7], polymers [8] for removal of mercury, but very few processes have been developed for removal of melamine. Granular activated carbon (GAC) is one of them. The limitation of these Separation techniques, they are time consuming, adsorption capacity is relatively low of these adsorbents. Lately, it was reported that thymine has functional group which can selectively bind Hg^{2+} and melamine [9]. Graphene has also been proven to be superior adsorbents for environmental applications in the removal of heavy metal ions and organic pollutants showing high adsorption capacity and selectivity due to its ultra-high surface area ($\geq$ 1000 m^2/g) and tailor able functionalities. [10,11]. So, fabrication of magnetic thymine will lessen the separation time and thymine functionalized graphene oxide will increase adsorption capacity of adsorbent and a new adsorbent nanomaterial for removal of melamine and mercury simultaneously.

1.2. Environmental Pollutant

Environmental pollution is one of the most serious problems facing humanity and other life forms on our planet today. Environmental pollution is defined as ~~"~~the contamination of the physical and biological components of the earth/atmosphere system to such an extent that normal environmental processes are adversely affected." Pollutants can be naturally occurring substances or energies, but they are considered contaminants when in excess of natural levels. Any use of natural resources at a rate higher than nature's capacity to restore itself can result in pollution of air, water, and

land. Pollution is a significant problem facing the environment. As the world's population continues to grow, so does the amount of potentially toxic substances that are released into the ecosystem. Environmental pollutants can be derived from a number of sources. Knowing what the different types of pollution are and where they come from can help you to understand the potential impact of these pollutants on your health and the health of the planet.

1.3 Heavy metal as pollutant

Heavy metals are defined as metallic elements that have a relatively high density compared to water [12]. With the assumption that heaviness and toxicity are inter-related, heavy metals also include metalloids, such as arsenic, that are able to induce toxicity at low level of exposure [13]. In recent years, there has been an increasing ecological and global public health concern associated with environmental contamination by these metals. Also, human exposure has risen dramatically as a result of an exponential increase of their use in several industrial, agricultural, domestic and technological applications [14]. Reported sources of heavy metals in the environment include gynogenic, industrial, agricultural, pharmaceutical, domestic effluents, and atmospheric sources [15]. Environmental pollution is very prominent in point source areas such as mining, foundries and smelters, and other metal-based industrial operations [12, 14, 15].

Although heavy metals are naturally occurring elements that are found throughout the earth’s crust, most environmental contamination and human exposure result from anthropogenic activities such as mining and smelting operations, industrial production and use, and domestic and agricultural use of metals and metal-containing compounds [15–18]. Environmental contamination can also occur through metal corrosion, atmospheric deposition, soil erosion of metal ions and leaching of heavy metals, sediment re-suspension and metal evaporation from water resources to soil and ground water [19]. Natural phenomena such as weathering and volcanic eruptions have also been reported to significantly contribute to heavy metal pollution [12, 14, 15, 18, 19]. Industrial sources include metal processing in refineries, coal burning in power plants, petroleum combustion, nuclear power stations and high-

tension lines, plastics, textiles, microelectronics, wood preservation and paper processing plants [20–22].

It has been reported that metals such as cobalt (Co), copper (Cu), chromium (Cr), iron (Fe), magnesium (Mg), manganese (Mn), molybdenum (Mo), nickel (Ni), selenium (Se) and zinc (Zn) are essential nutrients that are required for various biochemical and physiological functions [23]. Inadequate supply of these micro-nutrients results in a variety of deficiency diseases or syndromes [23].

Heavy metals are also considered as trace elements because of their presence in trace concentrations (ppb range to less than 10ppm) in various environmental matrices [24]. Their bioavailability is influenced by physical factors such as temperature, phase association, adsorption and sequestration. It is also affected by chemical factors that influence speciation at thermodynamic equilibrium, complexation kinetics, lipid solubility and octanol/water partition coefficients [25]. Biological factors such as species characteristics, tropicinteractions, and biochemical/physiological adaptation, also play an important role [26].

The essential heavy metals exert biochemical and physiological functions in plants and animals. They are important constituents of several key enzymes and play important roles in various oxidation-reduction reactions [23]. Copper for example serves as an essential co-factor for several oxidative stress-related enzymes including catalase, superoxide dismutase, peroxidase, cytochrome c oxidases, ferroxidases, monoamine oxidase, and dopamine β-monooxygenase [27–29]. Hence, it is an essential nutrient that is incorporated into a number of metalloenzymes involved in hemoglobin formation, carbohydrate metabolism, catecholamine biosynthesis, and cross-linking of collagen, elastin, and hair keratin. The ability of copper to cycle between an oxidized state, Cu (II), and reduced state, Cu (I), is used by cuproenzymes involved in redox reactions [27–29]. However, it is this property of copper that also makes it potentially toxic because the transitions between Cu (II) and Cu (I) can result in the generation of superoxide and hydroxyl radicals [27–30]. Also, excessive exposure to copper has been linked to cellular damage leading to Wilson disease in humans [29, 30]. Similar to copper, several other essential elements are required for biologic functioning, however, an excess amount of such metals produces cellular and tissue damage leading to a variety of adverse effects and human diseases. For some

including chromium and copper, there is a very narrow range of concentrations between beneficial and toxic effects [30, 31]. Other metals such as aluminum (Al), antinomy (Sb), arsenic (As), barium (Ba), beryllium (Be), bismuth (Bi), cadmium (Cd), gallium (Ga), germanium (Ge), gold (Au), indium (In), lead (Pb), lithium (Li), mercury (Hg), nickel (Ni), platinum (Pt), silver (Ag), strontium (Sr), tellurium (Te), thallium (Tl), tin (Sn), titanium (Ti), vanadium (V) and uranium (U) have no established biological functions and are considered as non-essential metals [31].

1.3.1. Heavy metal mercury as pollutant

Mercury is a highly toxic and widespread pollutant that comes from diverse sources including nature and human activities [33, 34]. The United States Environmental Protection Agency (EPA) has estimated that the total mercury released into the environment reaches to 7500 tons per year.

Figure 1.1. Image of mercury (Wikipedia)

Water-soluble divalent mercuric ion (Hg^{2+}) one of the most usual and stable forms of mercury pollution, can damage the brain, nervous system, kidneys, and endocrine system, resulting in often severe effects [35]. What is more, this element poses human risks even at relatively low dosages. Mercury shows high toxicity even at low concentrations [35-36] and exists in many metallurgical industry wastewater and releases into environments. Its non-biodegradable, fluidity, tends to accumulate in living tissues and easy transformed to methyl mercury force us to search for an effective method for removal of aqueous mercury.

1.4. Organic contaminants

Organic contaminants including dye, humic substances, phenolic compounds, petroleum, surfactants, pesticides, and pharmaceuticals are important pollutants in wastewaters. The presence of organic contaminants in water may produce toxic chemicals during disinfection. Among the contaminants, humic substances such as humic acid, fulvic acid, or humin, which result from the decay of organic matter and pharmaceuticals such as antibiotics, are most abundant in farm wastewaters; and these should be removed before discharge. Adsorption by zeolites has been found to be an effective technique for removing organic contaminants from wastewaters. However, modified zeolite (surfactant modification) is commonly used to remove organic contaminants from wastewaters (Wang and Peng, 2010).

Organic Contaminants Petroleum hydrocarbons (fuels)—benzene, toluene, xylene, polycyclic aromatics, MTBE.
Chlorinated solvents—trichloroethene, tetrachloroethene, trichloroethane, carbon tetrachloride.
Pesticides—DDT, toxaphene, atrazine Polychlorinated biphenyls—PCBs Coal tar—polycyclic aromatics, melamine etc.
Pharmaceuticals/food additives/cosmetics— drugs, surfactants, dyes
Gaseous compounds—CFCs (Freon), HCFCs

1.4.1 Hazardous effect of melamine

Melamine is the organic compound with the formula $C_3H_6N_6$. This white solid is a trimer of cyanamide, with a 1,3,5-triazine skeleton. It is widely used in the production of certain plastics, e.g. Formica. Like cyanamide, it contains 67% nitrogen by mass, and its derivatives have fire retardant properties due to its release of nitrogen gas when burned or charred.

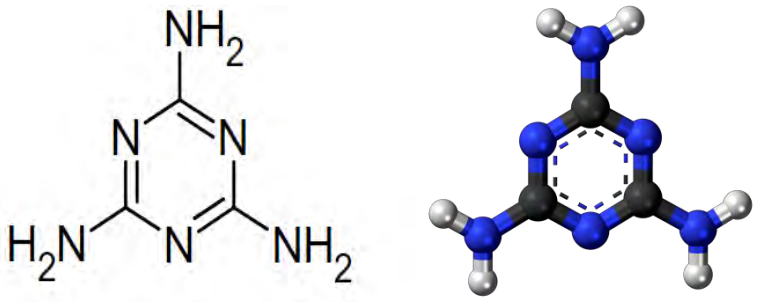

Figure 1.2. Structure of melamine

Melamine, which is a triazine heterocyclic organic compound, has been widely used in the production of plastics, coatings, flame retardants, melamine resins, and other products [37]. In the past years, melamine has been illegally and unethically added to food and animal feeds to increase its apparent crude protein content, because customary Kjeldahl protein analysis approach fails to distinguish the nitrogen sources of protein from that of non-protein [38]. However, the intake of melamine for human and animals could lead to the formation of insoluble complexes in kidney and subsequent tissue injury [39].

1.5. Removal of mercury (Hg^{2+})

There are many conventional methods for treatment of aqueous mercury such as ion exchange, [40,41] chemical precipitation [42], Filtration [43] coagulation [44] reduction, [45,46], membrane separation [47,48] and adsorption [49-51] have been widely applied in this field. Among those conventional methods, the adsorption method is considered as the most facile, and cost-effective [52].

1.5.1 Coagulation

Coagulation is an easy wastewater treatment method. In this method the addition of chemicals to change the physical state of solution and suspended solids and facilitate their removal by sedimentation. For a long time, the Coagulation method for treatment of dye-containing wastewater has been used as main method for its low capital cost [53, 54]. However, the generation of sludge and ineffective decolorization of some soluble dyes was the main limitation of this process [55, 56].

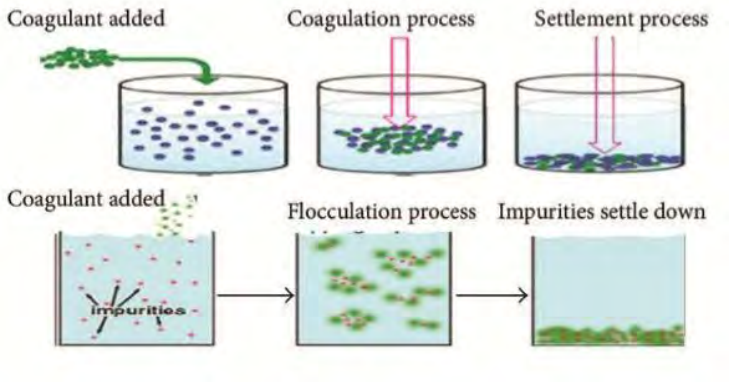

Figure 1.3. Schematic illustration of Coagulation process [56].

1.5.2 Filtration

Filtration is the most common methods in the filtration technology. Filtration methods such as ultrafiltration, nanofiltration and reverse osmosis have been used for water reuse and the chemical recovery [57,58]. In the textile industry, these filtration methods can be used for both filtering and recycling of not only pigment rich wastewaters, but also mercerizing and bleaching wastewaters. The specific temperature and chemical composition of the wastewaters determines the type and porosity of the filter to be applied. Further, the utilization of membrane technology for dye removal from textile wastewater is very effective as reported by various researchers [58, 59]. However, the main drawbacks of membrane technology are the high cost, frequent membrane fouling, requirement of different pretreatments depending upon the type of influent wastewaters, and production of concentrated dye-bath which further needs proper treatment before its safe disposal to the environment [60, 61]. For membrane filtration, proper pretreatment units for removing suspended solid of the wastewaters are almost mandatory to increase the life time of the membranes. These make the process more expensive and thereby limit the application.

1.5.3 Membrane separation

Membrane separation is a technology which selectively separates (fractionates) materials via pores and/or minute gaps in the molecular arrangement of a continuous structure. Membrane separations are classified by pore size and by the separation

driving force. These classifications are: Microfiltration (MF), Ultra filtration (UF), Ion-Exchange (IE), and Reverse Osmosis (RO).

Scale of separation

In the below figure are examples of variant substances shown in approximate correspondence to the pore size of the membrane separation method that may be employed.

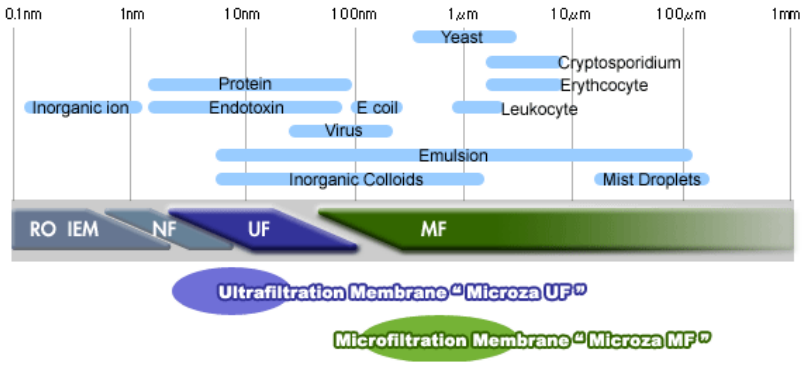

Figure 1.4. Scale of Membrane separation [60].

1.6. Removal of melamine

Very few methods have been developed for the efficient removal of melamine from aqueous solution. Advanced oxidation process (AOP) and GAC process have been commonly used for the removal of trace substances such as melamine.

1.6.1. Advanced oxidation process (AOP)

The AOP device used in the experiments, as shown in Fig. 1.5, consisted of a semi-batch device, with 1L capacity, and had the provision for stirring using a dosing pump. To prevent the target materials from being absorbed in the pipelines, tubes coated internally with Teflon were used, with corrosion prevented using SUS-316 and Teflon as materials for the ozone dissolving device and pipelines, respectively. Fixed quantities of ozone and peroxide were injected into an effect or via the automatic syringe device. The reaction time was 20 min and the experiments were carried out under the same conditions [62, 63].

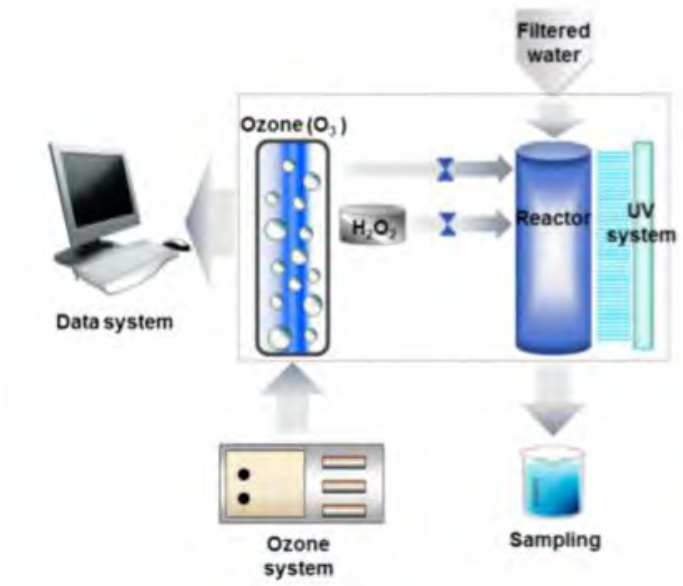

Figure 1.5. Schematic diagram of advanced oxidization process (AOP) [61].

1.6.2. Granular activated carbon (GAC) Process

Granular activated carbon is a specific preparation of activated carbon, or activated charcoal. It has been used as a purification agent since antiquity. Activated carbon was used for drinking water filtration in ancient India, and as a multi-use purifier in ancient Egypt. In modern times, it was introduced to Europe's sugar refining industry in the early 19th century. Today, activated carbon in various forms, including granular, is used in a wide range of industrial, commercial, and home applications to remove contaminants. The two most common options for locating a GAC treatment unit in water treatment plants are: (1) post-filtration adsorption, where the GAC unit is located after the conventional filtration process (post-filter contactors or absorbers); and (2) filtration-adsorption, in which some or all of the filter media in a granular media filter is replaced with GAC. Examples of these configurations are shown in Figures 1.6 and 1.7, respectively.

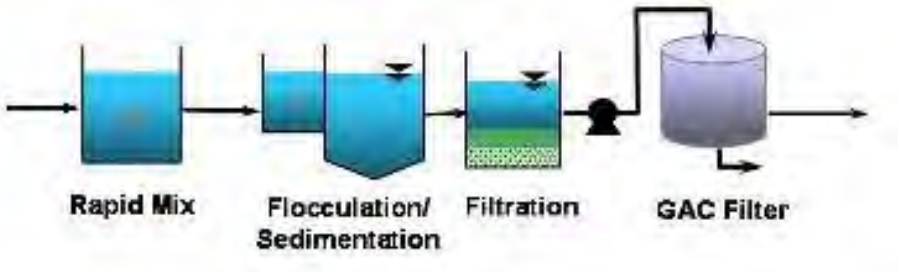

Figure 1.6. Post-filtration adsorption process of GAC [63].

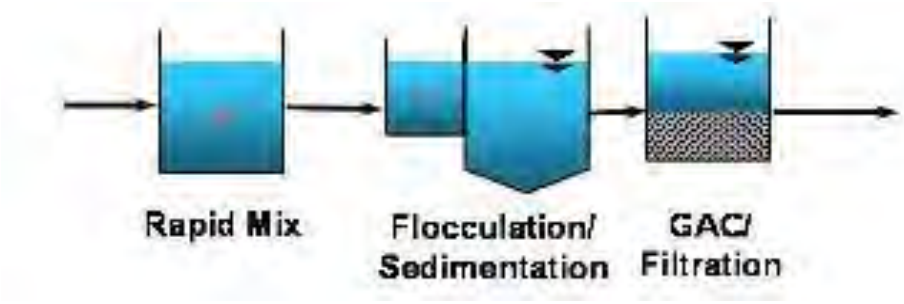

Figure 1.7. Filtration adsorption process of GAC [63].

1.7. Graphene Oxide as adsorbent

Graphene oxide (GO) is one of those materials - it is a single-atomic layered material, made by the powerful oxidation of graphite, which is cheap and abundant. Graphene oxide is an oxidized form of graphene, laced with oxygen-containing groups. It is considered easy to process since it is dispersible in water (and other solvents), and it can even be used to make graphene. Graphene oxide is not a good conductor, but processes exist to augment its properties. It is commonly sold in powder form, dispersed, or as a coating on substrates.

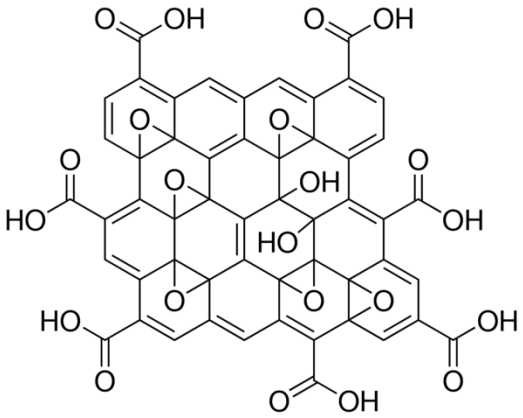

Figure 1.8. Structure of graphene oxide (GO)

Graphene oxide (GO) derived from graphene has received much attention over the past few years as a novel adsorbent substrate for various applications due to its outstanding features, such as large specific surface area, high water dispersibility, and good surface fictionalization feasibility. The unique structural and functional properties associated with graphene oxide (GO), such as its high mechanical strength (>1060 GPa), theoretical surface area (about 2600 m^2 g^{-1}) and the presence of hydroxyl and carboxylic groups are important characteristics that make graphene

oxide containing materials suitable for environmental applications [64]. For instance, some authors have employed these properties for adsorption of biphenol A [65] and arsenic, and heavy metal [66, 67] while others have employed the unique chemical and physical properties of iron magnetic nanoparticles together with other materials in the removal of some toxic substances from solution. [64, 66, 67].

1.8. Magnetic graphene oxide (MGO)

Magnetic nanoparticles (NPs) in the presence of graphite oxide (GO) has been investigated by varying the iron precursor dosage and reaction time (product donated as MP/GO). The synthesized magnetic NPs were anchored on the GO sheets due to the abundant oxygen-containing functionalities on the GO sheets such as carboxyl, hydroxyl and epoxy functional groups. The introduced NPs changed the intrinsic functionalities and lattice structure of the basal GO iron magnetic nanoparticles have the ease of being removed from solution by magnetization. Iron magnetic nanoparticles synergistically combined with other nanomaterials have very promising capacities for water treatment. With the foregoing in mind, the aim of this study was to covalently combine GO and iron magnetic nanoparticles into one chemical entity at reduced temperature, and employ this new material [68].

1.9 Interaction of thymine with melamine & mercury (Hg^{2+})

Thymine (T) is one of the bases in DNA. It is well known that thymine has a Specific binding with Hg (II) to form thymine-Hg (II)-thymine (T-Hg (II)-T). NMR Studies have demonstrated that Hg (II) binds directly to N-3 of two thymidine residues in place of two imino protons and forms N-Hg (II)-N bond [69]. Nowadays, Various researchers are committed to Hg (II) probes or sensors based on those specific interaction [70-72]. If we can combine graphene with thymine, capability of graphene selective removal of Hg (II) will improve.

Thymine possesses complementary NH---O and NH---N hydrogen bonds with melamine, which could be a good choice for melamine detection based on hydrogen bond-based strategy[73].

1.10 Our approach

There are many conventional methods for treatment of aqueous mercury such as ion exchange, [40,41] chemical precipitation [42], solvent extraction [43] coagulation, [44] reduction, [45,46], membrane separation [47,48] and adsorption [49-51] have been widely applied in this field. Among those conventional methods, the adsorption method is considered as the most facile, and cost-effective [52].

On the other hand, there are many adsorption techniques such as granular activate carbon (GAC) process, advanced process (AOP). But the problem of these processes, have complicated instrumentation, are expensive and real time testing are so difficult.

In this research, we wanted to synthesize a multifunctional nanomaterial which will act as an adsorbent. Thymine based magnetic graphene oxide have been synthesized for this purpose. We have synthesized this thymine based magnetic graphene oxide in two procedures. In first procedure we synthesized our adsorbent where we modified thymine for two times, and another procedure we modified thymine for the once. Thymine (T) is one of the bases in DNA. It is well known that thymine has a specific binding with Hg(II) to form thymine-Hg(II)-thymine (T-Hg(II)-T). NMR studies have demonstrated that Hg(II) binds directly to N-3 of two thymidine residues in place of two imino protons and forms N-Hg(II)-N bond[60].Thymine possesses complementary NH---O and NH---N hydrogen bonds with melamine [64]. Interaction of melamine and mercury with thymine shown in figure

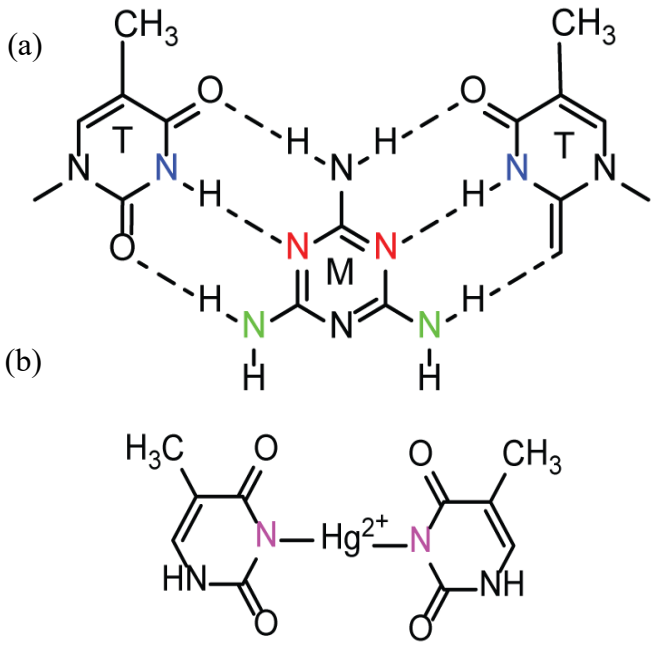

Figure 1.9 Interaction of (a) melamine with thymine and (b) mercury with thymine

Iron oxide shows ferromagnetism so incorporation with iron oxide nanoparticle (Fe_3O_4 NP) it will show magnetic property. Here we are using graphene oxide (GO), Graphene oxide (GO) derived from graphene has received much attention over the past few years as a novel adsorbent substrate for various applications due to its outstanding features, [56] such as large specific surface area, high water dispersibility, and good surface functionalization feasibility. So, enhance with graphene oxide will increase the adsorption capacity.

Thus, our synthesized thymine immobilized magnetic graphene oxide more effective and it could adsorb melamine and mercury simultaneously. For its magnetic property we able to separate it magnetically after adsorption of mercury and melamine from solution which is so easy process. Thymine grafting with the surface of silica coated Fe_3O_4 and graphene oxide increased the adsorption capacity of our material.

References

1. T.L. Fodey, R. Liu, L. Liu, S. Song, G. Cui, Q.Zheng, H. Kuang & C. Xu. ―Development of an optical biosensor based immunoassay to screen infant formula milk samples for adulteration with melamine,"*Anal. chem*., vol.83, pp. 5012–5016. 2011.
2. H. H. Harris, I. J. Pickering, G. N. George, ―The Chemical form of Mercury in Fish,"*Science.*,vol. 301,pp.1203−1203, 2003.
3. R. Reimschuessel & B. Puschner, ―Melamine toxicity-stones vs. crystals,"*J. Medical Toxicology.,*vol.6, pp. 468–469, 2010.
4. J. W. Sekowski, L. H. Malkas, Y. Wei, R. J. Hickey, ―Mercuric Ion Inhibits the Activity and Fidelity of the Human Cell DNA Synthesome," *Toxicol. Appl. Pharmacol*., vol. 145, pp. 268−276, 1997.
5. E. Climent, M. D. Marcos, R. Martinez-Manez, F. Sancenon, J. Soto, K. Rurack, P. Amoros, ―The Determination of Methylmercury in Real Samples Using Organically Capped Mesoporous Inorganic Materials Capable of Signal Amplification,"*Angew. Chem., Int. Ed*., Vol. 48, pp. 8519−8522, 2009.
6. Li, N. Bai, R. B. Liu, C. K. ―Enhanced and Selective Adsorption of Mercury Ions on Chitosan Beads Grafted with Polyacrylamide via Surface-Initiated Atom Transfer Radical Polymerization,"*Langmuir*., vol. 21, pp. 11780−11787, 2005.

7. G. ayramo lu, M. Y. Arica, ―Kinetics of Mercury Ions Removal from Synthetic Aqueous Solutions Using by Novel Magnetic p(GMAMMA-EGDMA) eads," *J. Hazard. Mater*., vol. 144, pp. 449−457, 2007.
8. Y. Uludag, H. . z belge, L. Yilmaz, ―Removal of mercury from aqueous solutions via polymer-enhanced ultra-filtration,"*J. Member. Sci*., vol. 129, pp 93−99, 2005.
9. N. Dave, M. Y. Chan, P. J. Huang, B. D. Smith, J. W. Liu, ―Regenerable DNA-Functionalized Hydrogels for Ultrasensitive, Instrument-Free Mercury (II) Detection and Removal in Water,". *J. Am. Chem*. *Soc.*, vol.132, pp.12668−12673, 2010.
10. H. Bai, C. Li, G. Shi. ―Functional composite materials based on chemically converted graphene,"*Adv. Mater*. vol. 23, pp. 1089−1115, 2011.
11. M.D. Stoller, S. Park, Y. Zhu, J. An, R.S. Ruoff.―Graphene-based ultracapacitors, *"Nano Lett*., vol. 8, pp. 3498−3502, 2008.
12. J.E, Fergusson editor. ―The Heavy Elements: Chemistry, Environmental Impact and Health Effects," *Oxford: Pergamon Press*., vol. 3, pp. 23, 1990.
13. J.H. Duffus ―Heavy metals-a meaningless term," *Pure Appl Chem*., vol. 74(5), pp. 793–807, 2002.
14. H, radl, editor. ―Heavy Metals in the Environment: Origin, Interaction and Remediation,"*London: Academic Press*., vol. 06, 2002.
15. Z.L He, X.E Yang, P.J Stoffella." Trace elements in agroecosystems and impacts on the environment*," J Trace Elem Med Biol*., vol.19 (2–3), pp.125–140, 2005.
16. R.A Goyer. Toxic effects of metals. In: C.D Klaassen, editor. ―Cassarett and Doull's Toxicology: The asic Science of Poisons," *New York: McGraw-Hill Publisher*., vol. 34, pp. 811–867, 2001.
17. N. Herawati, S. Suzuki, K. Hayashi, I.F Rivai, H. Koyoma, ―Cadmium, copper and zinc levels in rice and soil of Japan, Indonesia and China by soil type,"*BullEnvContamToxicol*., vol. 64, pp. 33–39, 2000.
18. S. Shallari, C. Schwartz, A. Hasko, Morel JL. ―Heavy metals in soils and plants of serpentine and industrial sites of Albania". *Sci Total Environ*., Vol.19209, pp. 133–142,1998.

19. J.O. Nriagu. ―A global assessment of natural sources of atmospheric trace metals,"*Nature*., vol.338, pp. 47–49, 1989.
20. A. Arruti, I. Fernández-Olmo, A. Irabien, ―Evaluation of the contribution of local sources to trace metals levels in urban PM2.5 and PM10 in the Cantabria region (Northern Spain),"*J Environ Monit*., vol. 12 (7), pp.1451–1458, 2010.
21. E. Sträter, A. Westbeld, O. Klemm. ―Pollution in coastal fog at Alto Patache, Northern Chile,"*Environ Sci Pollut Res Int*., bol. 03, pp. 67, 2010.
22. J.M. Pacyna, L.W. Chang, L. Magos, T. Suzuli, ―Monitoring and assessment of metal contaminants in the air," Toxicology *of Metals. Boca Raton, FL: CRC Press*.,vol. 89, pp. 9–28,1996.
23. WHO/FAO/IAEA. World Health Organization. Switzerland: Geneva.―*Trace Elements in Human Nutrition and Health,"* 1996.
24. T. Kabata- Pendia A 3rd, editor. ―Trace Elements in Soils and Plants,"*Boca Raton, FL: CRC Press*., vol. 89, pp. 83, 2001.
25. J.L. Hamelink P.F. Landrum, B.L. Harold, B.H. William, ―ioavailability: Physical, Chemical, and iological Interactions," *Boca Raton, FL: CRC Press Inc*., vol. 78, pp. 21, 1994.
26. J.A.S. Verkleji. ―The effects of heavy metals stress on higher plants and their use as biomonitors In Plant as Bioindicators: Indicators of Heavy Metals in the Terrestrial Environmen,t". *Markert B, editor. New York*: *VCH*., vol. 28, pp. 415–424, 1993.
27. B.R Stern. ―Essentiality and toxicity in copper health risk assessment: overview, update and regulatory considerations," *Toxicol Environ Health A*., vol. 73(2), pp. 114–127, 2010.
28. L.J. Harvey, H.J. McArdle. ―iomarkers of copper status: a brief update". *Br J Nutr*., Vol. 99(S3) :S, pp. 10–S13, 2008.
29. Agency for Toxic Substances and Disease Registry (ATSDR) Toxicological Profile for Copper. *Atlanta, GA: Centers for Disease Control*, 2002.
30. Tchounwou P, Newsome C, Williams J, Glass K. ―Copper-induced cytotoxicity and transcriptional activation of stress genes in human liver carcinoma cells," *Metal Ions Biol Med*., vol. 67, pp.10:285–290, 2008.
31. L.W. Chang, L. Magos, T. Suzuki, editors. Toxicology of Metals. *Boca Raton. FL, USA: CRC Press*., vol. 65, pp. 37-56, 1996.

32. H. H. Harris, I. J. Pickering, G. N. George, –The Chemical form of Mercury in Fish,"*Science.,* vol. 301, pp 1203−1203, 2003.
33. P. B. Tchounwou, W. K. Ayensu, N. Ninashvili, D. Sutton, –Environmental Exposure to Mercury,"*Environ. Toxicol*.,vol.18, pp. 149− 175,2003.
34. J. W. Sekowski, L. H. Malkas, Y. Wei, R. J. Hickey, –Mercuric Ion Inhibits the Activity and Fidelity of the Human Cell DNA Synthesome,"*Toxicol. Appl. Pharmacol*,. vol. 145, pp 268−276, 1997.
35. R. J. Qu, Y. Zhang, C. M. Sun, C. H. Wang, –Adsorption of Hg (II) from an Aqueous solution by silica-gel supported diethylenetriamine prepared via different routes: kinetics, thermodynamics, and isotherms,". *J. Chem. Eng*., vol. 55, pp. 1496, 2010.
36. S. T. Song, N. Saman, K. Johari, H. Mat, –Removal of Hg (II) from aqueous Solution by adsorption using raw and chemically modified rice straw as novel Adsorbents," *Ind. Eng. Chem. Res*,. vol. 52, pp. 13092, 2013.
37. T. L. Fodey, R. Liu, L. Liu, S. Song, G. Cui, Q.Zheng, H. Kuang & C. Xu. –Development of an optical biosensor based immunoassay to screen infant formula milk samples for adulteration with melamine,"*Anal. chem*.,vol.83,pp. 5012–5016. 2011
38. T. Sanji, –Fluorescence –turn-on" detection of melamine with aggregation-induced-emission-active tetraphenylethe,"*Chem. Eur. J.,* vol.18, pp. 15254–15257, 2012.
39. R. Reimschuessel, & B. Puschner, –Melamine toxicity-stones vs. crystals," *J. Medical Toxicology,*vol. 6, pp. 468–469, 2010.
40. S. Chiarle, M. Ratto, M. Rovatti, –Mercury removal from water by ion exchange resins adsorption,"*Wat. Res*., vol. 11, pp. 2971, 2000.
41. A. Oehmen, D. Vergel, J. Fradinho, M. A. M. Reis, –Mercury removal from water streams through the ion exchange membrane bioreactor concept,"*J. Hazard. Mater*., vol. 264, pp. 65, 2014.
42. U. Skyllberg, A. Drott, Competition between disordered iron sulfide and natural organic matter associated thiols for mercury (II)-an EXAFS study. Environ. *Sci. Technol*. 2010, 44, 1254.
43. S. A. Idris, S. R. Harvey, L. T. Gibson. Selective extraction of mercury (II) from water samples using mercapto functionalised-MCM-41 and regeneration

of the sorbent using microwave digestion. *J. Hazard. Mater*., vol. 93, pp. 171, 2011.

44. Y. K. Henneberry, T. E. C. Kraus, J. A. Fleck, D. P. Krabbenhoft, ―Removal of inorganic mercury and methylmercury from surface waters following coagulation of dissolved organic matter with metal-based salts," Sci. *Total. Environ*., vol.409, pp.631, 2011.
45. R. Stolle, H. Koeser, H. Gutberlet, ―Oxidation and reduction of mercury by SCR DeNOx catalysts under flue gas conditions in coal fired power plants," *Appl. Catal. B.Environ*," vol. 144, pp. 48, 2014.
46. A. M. Berkovic, S. G. Bertolotti, L. S.; Villata, M. C. Gonzalez, ―Photoinduced reduction of divalent mercury by quinones in the presence of formic acid under anaerobic conditions,"*Chemosphere*. vol. 89, pp. 1189 2013.
47. K. Chakrabarty, P. Saha, A. K. Ghoshal, ―Separation of mercury from its aqueous solution through supported liquid membrane using environmentally benign diluents," J. *Membrane. Sci*., vol. 350, pp.395, 2010.
48. K. Chakrabarty, P. Saha, A. K. Ghoshal, ―Simultaneous separation of mercury and lignosulfonate from aqueous solution using supported liquid membrane. Elemental mercury oxidation and adsorption on magnesite powder modified by Mn at low temperature,"*J. Membrane. Sci*., vol. 346, pp. 37, 2010.
49. Y. L. Xu, Q. Zhong, X. Y. Liu, ―Elemental mercury oxidation and adsorption on, magnesite powder modified by Mn at low temperature,". *J. Hazard. Mater*. vol. 283, pp. 252, 2015.
50. F. Di Natale, A. Erto, A. Lancia, D. Musmarra, ―Mercury adsorption on granular activated carbon in aqueous solutions containing nitrates and chlorides,"*J.Hazard. Mater*., vol. 192, pp.1842, 2011.
51. S. Wang, M. H. Wei, Y. M. Huang, ―iosorption of multifold toxic heavy metal ions from aqueous water onto food residue eggshell membrane functionalized with ammonium thioglycolate,"*J. Agric. Food Chem*., vol. 61, pp. 4988, 2013.
52. J. Wang, B. L. Deng, H. Chen, X. R. Wang, ―Removal of aqueous Hg (II) by polyaniline: sorption characteristics and mechanisms,"*Environ. Sci. Technol*., vol. 43, pp. 5223, 2009.

53. Y. Anjaneyulu, N.S Chary, and D.S.S. Raj, "Decolourization of industrial effluentsavailable methods and emerging technologies-a review,"*Reviews in Environmental Science and Biotechnology*., vol. 4, pp. 245-273, 2005.
54. V. Golob, A. Vinder, and M. Simonic, "Efficiency of coagulation/flocculation method for treatment of dye bath effluents,"*Dyes and Pigments*.,vol. 67, pp. 93-97, 2005.
55. F.I., Hai, K. Yamamoto, and K.Fukushi, "Hybrid treatment systems for dye wastewater," *Critical Reviews in Environmental Science and Technology*., vol. 37, pp. 315-377, 2007.
56. M. Marcucci, G. Nosenzo, G. Capannelli, I. Ciabatti, D. Corrieri, and G. Ciardelli, "Treatment and reuse of textile effluents based on new ultrafiltration and other membrane technologies,"*Desalination*.,vol.138,pp.75-82, 2001.
57. C. Fersi, and M. Dhahbi, "Treatment of textile plant effluent by ultrafiltration and/ or nanofiltration for water reuse," *Desalination*., vol. 222, pp. 263-271, 2008.
58. S. Ledakowicz, M. Solecka, and R.Zylla, "iodegradation, decolourisation and detoxification of textile wastewater enhanced by advanced oxidation processes,"*Journal of Biotechnology*., vol. 89, pp. 175-184, 2001.
59. A.L. Ahmad, W.A Harris, and B. S. SyafiieOoi, "Removal of dye from wastewater of textile industry using membrane technology," *Universiti Teknologi Malaysia Jurnal Teknologi*., vol. 36 (F), pp. 31-44, 2002.
60. T. Robinson, G. Mcmullan, R. Marchant, and Nigham, P."Remediation of dyes in textile effluent: a critical review on current treatment technologies with proposed alternatives," *Bioresource Technology*.,vol. 77, pp. 247-255, 2001.
61. A. Akbari, S. Desclaux, J.C. Rouch, P. Aptel, and J.C. Remigy, "New UVphotografted nanofiltration membranes for the treatment of colored textile dye effluents," *Journal of Membrane Science*., vol. 286, pp. 342-350, 2006.
62. A. ach, G. Zelmanov, R. Semiat, "Wastewater mineralization using advanced oxidation process, Desalin," *Water Treat*., vol. 6, pp. 152–159, 2009.
63. E.C. Pires, T.J. Momenti."Combination of an anaerobic process with O_3, UV and O_3/UV for cellulose pulpbleaching effluent treatment, Desalin," *Water Treat*., vol. 5, pp. 213–222, 2009.

64. P.N. Diagboya, B.I. Olu-Owolabi, D. Zhou, B.H. Han, –Simultaneous sorption and reduction of U(VI) on magnetite–reduced graphene oxide composites investigated by macroscopic, spectroscopic and modeling techniques," *Carbon, Carbon*., vol. 79, pp. 174–182, 2014.
65. J. Xu, L. Wang, Y. Zhu, "Decontamination of Bisphenol A from Aqueous Solution by Graphene Adsorption," *Langmuir*., vol. 28, pp. 8418-8425 (2012).
66. V. Chandra, J. Park, Y. Chun, J.W. Lee, I.C. Hwang, K.S. Kim, –Water-dispersible magnetite-reduced graphene oxide composites for arsenic removal," *ACS Nano*., vol.4, pp. 3979-86, 2010.
67. A.K. Mishra, S. Ramaprabhu, –Water desalination with a single-layer MoS2 nanopore," *Desalination*, Vol.282, pp. 39-45 (2011).
68. S.R. Kanel, D. Nepal, B. Manning, H. Choi, "Dispersion and stability of bare hematite nanoparticles: effect of dispersion tools, nanoparticle concentration, humic acid and ionic strength," *J. Nanoparticle Res*., vol. 9, pp. 725-735 (2007).
69. I.N. Savina, C.J. English, R.L. Whitby, Y. Zheng, A. Leistner, S.V. Mikhalovsky, –A simple method for the production of large volume 3D macroporous hydrogels for advanced biotechnological, medical and environmental applications"., *J. Haz. Mater*., vol. 192, pp. 1002-1008, 2011.
70. Y. Tanaka, S. Oda, H. Yamaguchi, Y. Kondo, –15N-15N J-Coupling across Hg(II): direct observation of Hg(II)-mediated T-T base pairs in a DNA duplex,"*J. Am. Chem. Soc*., vol. 128, 2172, 2006.
71. C. C. Chang S. H. Lin, S. C. Wei, C. Y. Chen, –An amplified surface plasmon resonance –turn-on" sensor for mercury ion using gold nanoparticles,"*J. Am. Chem. Soc*., vol. 30, 235, 2011.
72. H. Wang, Y. X. Wang, J. Y. Jin, –Gold nanoparticle-based colorimetric and –turn-on" fluorescent probe for mercury(II) ions in aqueous solution,"*Anal. Chem*. vol. 80, pp. 9021, 2008.
73. X. J. Liu, C. Qi, T. Bing, X. H. Cheng, –Specific mercury (II) adsorption by thymine-based sorbent," *Talanta*., vol. 78, 253, 2009.

CHAPTER 2

Experimental

2.1 Materials and instruments

2.1.1 Chemicals and reagents

The chemicals and reagents used in this research were analytical grade and used without further purification. Deionized water was used as solvent to prepare most of the solutions of this work. The chemicals and reagents which were used in this research are given below:

i. Ethanol (99.8%) (Merck, Germany)
ii. Toluene (99.6%) (Merck, Germany)
iii. Methanol (99.0%) (Merck, India)
iv. N, N-dimethyl formamide (DMF)(Merck, Germany)
v. Iron (II) chloride(Merck, Germany)
vi. Sulphuric acid (98%) (Merck, Germany)
vii. Mercury(II) chloride(Merck, Germany)
viii. 11-Bromo-1-undecene(Sigma-Aldrich)
ix. Acetone (Sigma-Aldrich)
x. Trimethoxysilane (Sigma-Aldrich)
xi. Melamine (Sigma-Aldrich)
xii. Platinum chloride hydrate (99.9%) (H_2PtCl_6) (Merck, Germany)
xiii. Iron (III) chloride (Merck, Germany)

2.1.2 Instruments

Analysis of the samples was performed using the following instruments:

i. Fourier Transform Infrared Spectrophotometer (SHIMADZU FTIR-8400)
ii. Field Emission Scanning Electron Microscopy (JSM-7600F, Tokyo, Japan)
iii. X-ray Diffract meter (Philips, Expert Pro, Holland)
iv. X-ray photoelectron Spectroscopy (XPS)
v. Centrifuge machine (Hettich, Universal 16A)
vi. pH meter (Hanna, HI 8424, Romania)
vii. Digital Balance (AB 265/S/SACT METTLER, Toleto, Switzerland)
viii. Freeze dryer (Heto FD3)
ix. Oven (Lab Tech, LDO-030E)
x. UV-visible Spectrophotometer (Shimadzu-1800)

2.2 Method of preparation

2.2.1 Synthesis of graphene oxide (GO)

Graphene oxide (GO) was synthesized from graphite flake via modified Hummers method [1]. In brief 2 g graphite and 1.5 g $NaNO_3$ were mixed in a 500 mL round bottom flask in an ice water bath. 150 mL H_2SO_4 was slowly added with the mixture under mechanical stirring. Then, 9 g $KMnO_4$ was added to the mixture over about 1 h. During the addition of $KMnO_4$ ice water bath and stirring were maintained. Ice water bath was kept for another 2 h after the addition of $KMnO_4$. After 2 h ice water bath was removed while the stirring was continuing vigorously for 5days at room temperature. Then, 6 mL $H_2O_2$was added in to the mixture with another 2 h more. A solution was made mixing with deionized (DI) water 250 mL, H_2SO_4 (98%, 7.5 mL) and H_2O_2 (30 wt%, 4.20 mL). It was added to dilute and wash the mixture. Then the resulted mixture was washed by DI water and centrifuged and finally dialyzed for 5 days. The GO aqueous solution was dried by a freeze drier and in the end fluffy black dried GO was obtained.

2.2.2 Synthesis of iron oxide (Fe_3O_4) nanoparticle

The magnetite (Fe_3O_4) nanocrystals were prepared by chemical co-precipitation method [2]. An iron salt solution was obtained by mixing 0.005 mol $FeCl_3$ and 0.0025 mol $FeCl_2$ in 50 ml deoxygenated distilled water, such that Fe^{3+}/Fe^{2+} = 2 in molar. Twenty mL of 1.5 M NaOH was rapidly poured into the ferric salt solution under magnetic stirring at room temperature (RT). A black precipitate instantly formed. After continuously stirring for 10 min, the precipitate was separated by centrifugation and washed with the deoxygenated distilled water four times, followed with the deoxygenated anhydrous ethanol once, then vacuum-dried at 50 ˚C overnight, and we got the naked Fe_3O_4 nanocrystals were obtained as the control sample.

2.2.2.1 Synthesis of silica coated iron oxide (Fe_3O_4) nanoparticle

Silica coated Fe_3O_4 nanocrystals were produced by hydrolysis of TEOS on the surfaces of the magnetic Fe_3O_4 nanocrystals. After washing with the anhydrous ethanol in step 1, the precipitate Fe_3O_4 was ultrasonically redispersed in a solution containing 240 ml ethanol and 60 ml water, then loaded into a three-necked bottle. The pH value was adjusted to 9 with an ammonia solution and 4 ml TEOS was added under vigorous stirring. After 10 h, the ferrofluid was heated at 50 ˚C to further hydrolyses for another 12 h. The particles were again separated magnetically by a magnet bar and washed with the deoxygenated distilled water and anhydrous ethanol, then vacuum-dried at 50 ˚C overnight. The silica-coated Fe_3O_4 nanocrystals were prepared.

2.2.3. Preparation of 1-trimethoxysilylundecyl-thymine (1-TMSU-T)

Anhydrous toluene (5 mL) was introduced into a round-bottomed flask charged with I-U-T (278 mg, 1 mmol) and hydrogen hexachloroplatinate (IV) hydrate (~ 10 mg) under argon. Trimethoxysilane (0.3mL, 293 mg 2.4 mmol) was introduced into the mixture under argon using hypodermic syringe and the moisture was stirred at 70 ^{o}C for 16 h. After Cooling to room temperature, the mixture was immediately filtered through cotton fiber by applying argon pressure. Upon concentrating the filtrate, 1-TMSU-T was obtained as pale-yellow oil. [3]

2.2.4. Fabrication of magnetic thymine (MT)

0.1 g of Silica coated Iron oxide nanocrystal was added to a 25 mL flask containing a solution of respective trimethoxysilane in toluene (4 mL, 40 mM). This slurry was stirred for 4 h at room temperature. Then washed by toluene and separated magnetically by a magnet bar. Then washed by methanol. Dried at temperature 50 ^{o}C for 12 hours.

2.2.5. Fabrication of thymine immobilized graphene oxide functionalized magnetic thymine (MTGOT)

Magnetic thymine (0.1 g) and graphene oxide GO (0.1 g) were introduced in a flask containing 30-40 mL water. Then dispersed it ultrasonically and took it to a 50 mL of teflon bar and kept it into an autoclave. Keeping the temperature 190-200 ^{o}C for 5 hours. Hydrothermal reaction occurs here. After cooling it at room temperature we got MTGO which was washed several times by water. 0.1 g of MTGO was introduced in a 25 mL round bottom flask containing 1-TMSU-T (4 mL, 40 mM) toluene solution then reflux it for 12 hours at temperature of 110-115 ^{o}C. After cooling it at room temperature we washed it by DCM. Then vacuum-dried over night at temperature 100 ^{o}C [3].

2.2.6 Fabrication of thymine immobilized magnetic graphene oxide (MGOT)

Silica coated iron oxide (0.1 g) and graphene oxide GO (0.1 g) were introduced in a flask containing 30-40 mL water. Then dispersed it ultrasonically. Then took it to a 50 mL of Teflon bar and kept it into an autoclave. Keep it at temperature 190-200 ^{o}C for 5 hours. Hydrothermal reaction occurs here. After cooling it at room temperature we get MTGO which was washed several times by water. 0.1 g of MTGO was introduced in a 25 mL round bottom flask containing 1-TMSU-T (4 mL, 40 mM) toluene solution then reflux it for 12 hours at temperature of 110-115 ^{o}C. After cooling it at room temperature we washed it by DCM. Then dried over night at temperature 100 ^{o}C [4].

2.3 Sample characterization

2.3.1 Fourier transform infrared (FTIR) analysis

The infrared spectra of the silica coated iron oxide (Fe_3O_4) nanoparticle, magnetic graphene oxide (MGO), Thymine immobilized magnetic graphene oxide (MGOT) and Thymine Immobilized Graphene Oxide functionalized magnetic thymine (MTGOT) were recorded on an FTIR spectrometer in the region of 4000 – 500 cm^{-1}. All the 4-sample had dried. A small portion of samples were taken into vial and oven dried at 60^{o}C to confirmed their dryness. GO flake is very strong so it was grinded into a mortar with a pestle to get GO powder. Other three samples were not grinded because they were physically granule/powder in shape after completely drying. The

powder mixture was then compressed in a metal holder under a pressure of 8–10 tons to make a pellet. The pellet was then placed in the path of IR beam for measurements.

2.3.2 Field emission scanning electron microscopy (FE-SEM)

The surface morphology of the synthesized magnetic thymine (MT), thymine immobilized magnetic graphene Oxide (MGOT) and thymine immobilized graphene oxide functionalized magnetic thymine (MTGOT) was adopted using Field Emission Scanning Electron Microscopy (FE-SEM). The completely air-dried samples were put on a conducting carbon strip. The sample loaded strip was then mounted to a chamber that evacuated to ~ 10^{-3} to 10^{-4} torr and then a very thin platinum layer (~few nanometers thick) were sputtered on the sample to ensure the conductivity of the sample surface. The sample was then placed in the main SEM chamber to view its surface. The microscope was operated at an accelerating voltage of 5.0 kV. The system was computer interfaced and thus provides recording of the surface images in the computer file for its use as hard copy.

2.3.3 X-ray photoelectron spectroscopy (XPS)

XPS measurements were performed on samples that had been prepared within 4 days using the AXIS ULTRA spectrometer (Kratos Analytical). The base pressure in the analytical chamber was <3 x10^{-8} Pa. The monochromatic AlKα source (hν =1486.6 eV) was used at a power of 210 W. The photoelectron exit angle was 90^{o}, and the incident angle was 35.3^{o} from the plane of the surface. The analysis spot was 400 x 700 μm. The resolution of the instrument was 0.55 eV for Ag 3d peaks. Survey scans were collected for binding energies from 1100 to 0 eV with an analyzer pass energy of 160 eV and a step of 0.35 eV. The high-resolution spectra were run with a pass-energy of 20 eV and a step of 0.1 eV. Relative sensitivity factors (RSFs) for different elements were as follows: 1 for F (1s), 0.477 for N (1s), 0.955 for Br (3d). Only one set of XPS scans was performed on a given sample; therefore, XPS analysis before and after surface reactions were performed on different samples.

2.3.4 X-ray diffraction (XRD)

The crystallinity of magnetic thymine (MT) and MTGOT composite were analyzed by X-ray diffraction pattern in the powder state. The powder samples were pressed in a square aluminum sample holder (40 mm × 40 mm) with a 1 mm deep rectangular hole (20 mm x 15 mm) and pressed against an optical smooth glass plate. The upper surface of the sample was labeled in the plane with its sample holder. The sample holder was then placed in the diffracts meter.

2.3.5 Magnetic property analysis

The magnetic properties of bare iron oxide (Fe_3O_4), magnetic thymine (MT) thymine immobilized magnetic graphene Oxide (MGOT) and thymine immobilized graphene oxide functionalized magnetic thymine (MTGOT) were measured EV-9 micro sense (Germany) with an applied field between -10000 and 10000 Oe at room temperature.

2.3.6 Melamine adsorption experiments

A 8 mg portion of MTGOT and MGOT nanocluster adsorbent were dispersed in 10 mL of DI water (pH = 6.4) Separately. Then 10 mL of Melamine aqueous solution (100 mg/L) added to it under stirring. Then we separated 2 ml for each time separate it magnetically then added 2 ml of Methyl red (10 mg/L) for several times. Gradually concentration of Melamine decreases by adsorption. The adsorption process was monitored by measuring the changes in the absorbance at 427 nm at different time (i.e. 0 min, 1 min, 2 min, 5min, 6min, 10 min, 20 min, 30 min, 60 min, and 120 min.) with a UV−Vis spectrophotometer. The same experiment was repeated at same process twice.

2.3.7 Mercury adsorption experiment

The mercury removal experiments were carried out by using a Tekran 2500 Cold Vapor Atomic Adsorption Spectrophotometer (CVAAS) [9]. The details about CVAAS measurement setup are given in Scheme 2.1 (Supporting Information). The adsorption was done ai the p^H 5. In the time range of 5 to 180 Batch equilibrium

adsorption procedure was used to determine the Hg^{2+} adsorption minutes using a mercury solution 5 ml of 35 mg/L and 5 mg of MTGOT and MGOT for each time. Then we separate our adsorbent magnetically and measured the concentration of melamine by CVAAS.

References

1. Hummers, William S.; Offeman, Richard E. "Preparation of Graphitic Oxide". *J. Am. Chem. Soc*., vol. 80 (6), pp 1339, March 20, 1958.
2. Y.P He, S.Q Wang, C R Li, Y.M Miao, Z.Y Wu and B.S Zou. "Synthesis and characterization of functionalized silica-coated Fe_3O_4 super para magnetic nanocrystals for biological applications," *J. Phys. D: Appl. Phys., vol.* 38, pp. 1342, 2005.
3. J.S, Park, G. S. Lee, Y.J. Lee, Y.S. Park, and K. B. Yoon al." Organization of microcrystals on glass by adenine- thymine hydrogen bonding," *J. Am. Chem. Soc*., vol.124 (45), p.p. 13366-13367, 2002.
4. H.J. Kim, D.S. Park, M.H. Hyun, Y.-B. Shim, "Determination of Hg II Ion with a 1,11-Bis(8-quinoyloxy)-3,6,9-trioxaundecaneModified Glassy Carbon Electrode Using Spin-Coating Technique," *Electrocatalysis.,* vol.10, 303−306, 2007.
5. F. A. Jumeri, H. N. Lim, S. N. Arif fin, N. M. Huang, "Microwave synthesis of magnetically separable $ZnFe_2O_4$-reduced graphene oxide for wastewater treatment," *Ceram. Int.*, vol. 40, p.p.7057, 2014.
6. L. A. Al-Khateeb, S. Almotiry, M. A. Salam, "Adsorption of pharmaceutical pollutants onto graphene nanoplatelets," *Chem. Eng. J.,* vol. 248, p.p. 191, 2014.
7. Q. H. Wu, C. Feng, C. Wang, Z. Wang, "A facile one-pot solvothermal method to produce superparamagnetic graphene-Fe_3O_4 nanocomposite and its application in the removal of dye from aqueous solution,"*Coll. Surface*., vol. 101, p.p. 210, 2013.
8. S.Yang, T.Zeng. "Preparation of Graphene Oxide Decorated Fe_3O_4@SiO_2 Nanocomposites with Superior Adsorption Capacity and SERS Detection for Organic Dyes*," Journal of Nanomaterials.,* vol. 2015, p.p. 8, 2015.
9. R. T. Shandra and K. D. Sahally. "Visual detection and determination of melamine using synthetic dyes," *Journal of Applied chemistry*., vol. 2014, p.p. 7, 2014.

10. Y. Liu, D. J. A. Kelly, H. Yang, C. C. Lin, H.; Kuznicki, S. M.; Xu, Z. Novel. "Regenerable Sorbent for Mercury Capture from Flue Gases of Coal-Fired Power Plant," *Environ. Sci. Technol*., vol. 42 (16), p.p. 6205-6210, 2008.

CHAPTER 3

Results and Discussion

3.1 Fabrication of thymine Immobilized graphene Oxide functionalized magnetic thymine MTGOT and MGOT

Iron oxide nanoparticle (Fe_3O_4 NP) was synthesized via chemical co-precipitation method. This reaction was carried out using deoxygenated water by passing N_2 gas so that produced magnetic iron oxide cannot come contact with air. If those nanoparticles come in contact with air, it oxidized to Fe_2O_3. As a result the amount of Fe_3O_4 decreases and impurity incorporate which affect the further treatment For this reason coating of nanoparticle is essential the work was done by coating with silica using tetraethylorthosilicate (TEOS) in basic medium (25% of NH_3 solution) Anhydrous ethanol was used for controlling the reaction and for this case two steps reaction was carried out. In the first step, after addition of TEOS 10 hour without heat. Next step was carried out applying heat for 12 hours so that Si-O-Si bond break down and form Si-OH on the surface of Fe_3O_4 and completely coated. Reflux with 1-trimethoxysilylundecyl-thymine (1-TMSU-T), the reactive part of thymine derivative is silane that breaks Si-OH and new bond forms. Hydrothermal treatment with graphene oxide (GO) which would act as the scaffold to carry all the functional components. graphene oxide sheets were assembled on the magnetic thymine through electrostatic interactions Then for the second time reflux with 1-trimethoxysilylundecyl-thymine (1-TMSU-T) the active part silane can replace graphene oxides epoxy group and OH group form (Si-O-C) which can be assured by FTIR we found our desired compound thymine immobilized graphene Oxide functionalized magnetic thymine (MTGOT).

In this research we have synthesized a thymine based magnetic mesoporous silica with graphene oxide of mesoporous silica coating on iron oxide nanoparticle and graphene oxide nanosheet could enlarge the surface area, enhance the hydrophilicity and dispersity. Also, this hybrid material could be more easily functionalized. Besides, the Decorating Fe_3O_4 nanoparticles on GO nanosheets will impart the desirable magnetic property into graphene for adsorption process. On the other hand, reflux with 1-trimethoxysilylundecyle-thymine grafting with the surface

of magnetic graphene Oxide improves the dispersity of nanoparticles in aqueous medium. Overall synthesis has been showed in fig. 3.1

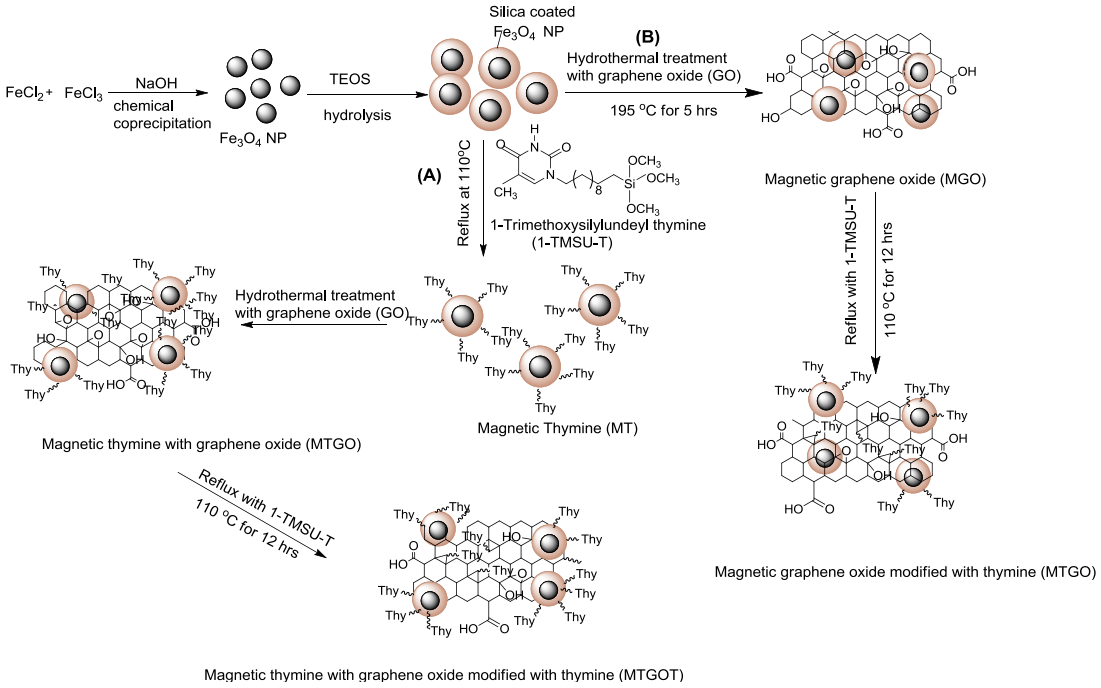

Figure 3.1 Schematic fabrication of thymine immobilized magnetic graphene oxide functionalized magnetic thymine MTGOT and MGOT

3.2 Functional group analysis using Fourier Transform Infrared spectroscopy (FTIR)

FTIR measurement were carried out in order to confirm the presence of functional groups on the surface of iron oxide nanoparticle (Fe_3O_4 NP), MGO, MGOT, and MTGOT measurements were carried out to detect the presence of functional groups on the surface of FTIR spectra of the silica-coated Fe_3O_4 nanocrystal The Si–O–Si bond's asymmetric stretching vibration at 1088.1cm^{-1} and symmetric stretching which indicates that the silica has successfully coated the surface of Fe_3O_4 nanocrystal by hydrolysis of TEOS. The absorption bands at about 3427.8 and 1637.6 cm^{-1} in all the spectra mainly originate from the –OH vibrations in H_2O.

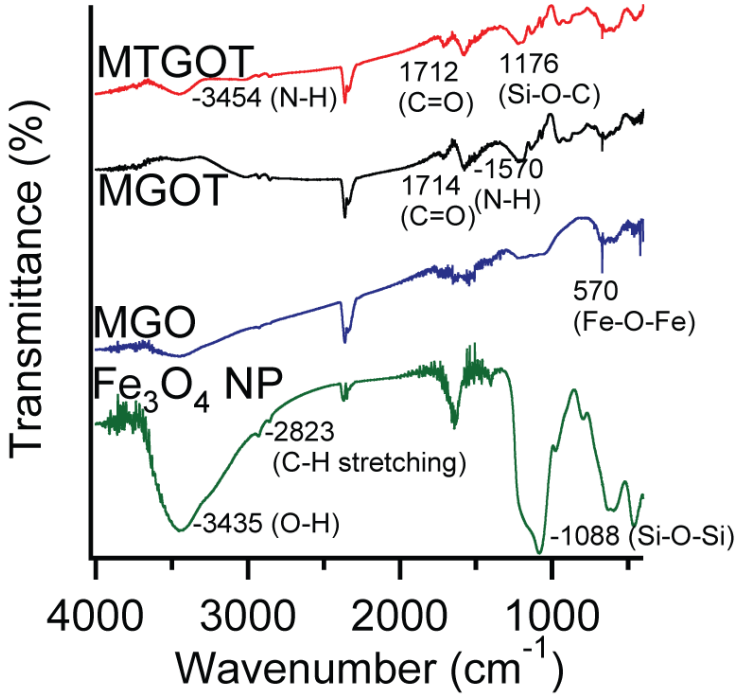

Figure 3.2 FTIR spectra of the Fe_3O_4 nanocrystals, Magnetic Graphene oxide (MGO), Thymine Immobilized Magnetic Graphene Oxide (MGOT) and Thymine Immobilized Graphene Oxide functionalized magnetic Thymine (MTGOT).

For the Fe_3O_4 nanoparticles, the peak at 581 cm^{-1} was indicative of the Fe−O−Fe vibrations. After reflux with 1-TMSU-T the peak at 1712 cm^{-1} and 1714 cm^{-1} of MGOT and MTGOT confirms that thymine has been successfully modified in the surface of MGO and MTGO.

Table 3.2 Characteristic peak and interpretations correspond to MTGOT and MGOT composite.

Wavenumber (cm^{-1})	Interpretations
570	Fe-O-Fe
1088	Si-O-Si
3568	N-H bending
1570	N-H stretching
1712-1714	C=O stretching
1180-1360	C-N stretching
3610-3640	O-H stretching

3.3 Surface morphology study using Field Emission Scanning electron microscope (FE-SEM)

Surface morphology of synthesized magnetic thymine (MT), MGOT and MTGOT were investigated be FE-SEM analysis.

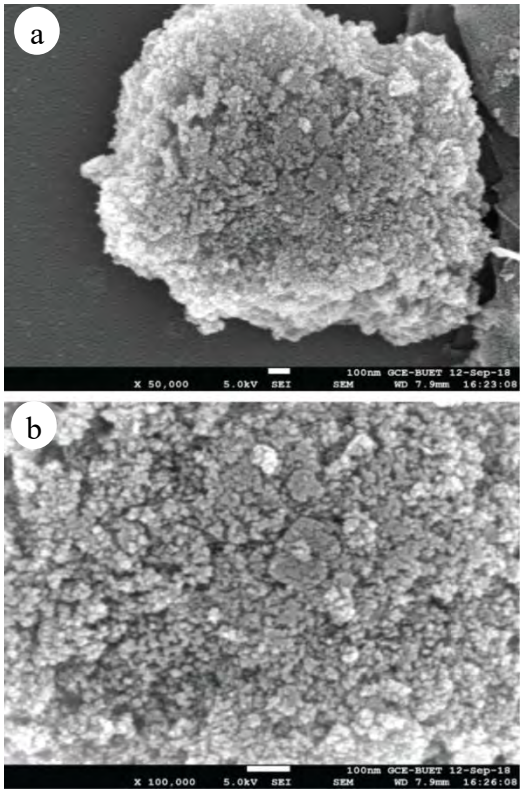

Figure 3.3. SEM images of MTGOT composite (a) resolution x50000 (b) resolution x100000

Fig. 3.3. shows the spherical structure of Fe_3O_4 with a smooth surface and wrinkled edge. Silica coated Fe_3O_4 nanoparticles with diameters of approximately 20 nm can be observed in the SEM image of magnetic thymine (MT) (Fig. 3.5), confirming the successful decoration of the magnetic nanoparticles on the surface of GO. The SEM image of magnetic thymine reveals that the silica nanoparticles were clearly coated on both sides of MGO. The change in morphology of silica coated iron oxide nanoparticle after modification with the thymine suggests the successful synthesis of the nanocomposite (Fig.3.4.). These results indicate that the GO sheets can function as a robust support and spacer for the decoration of the Fe_3O_4 nanoparticles and Thymine The existence of O, C, N, Fe and Si elements in the nanocomposite was confirmed by EDS pattern analysis as shown in (Fig.3.6).

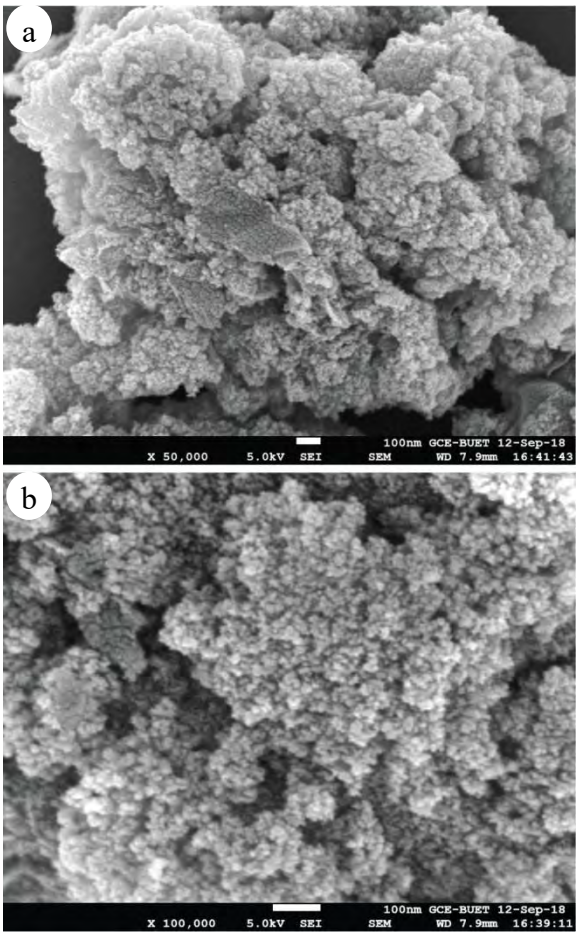

Figure 3.4. SEM images of MGOT composite (a) resolution x50000 (b) resolution x100000.

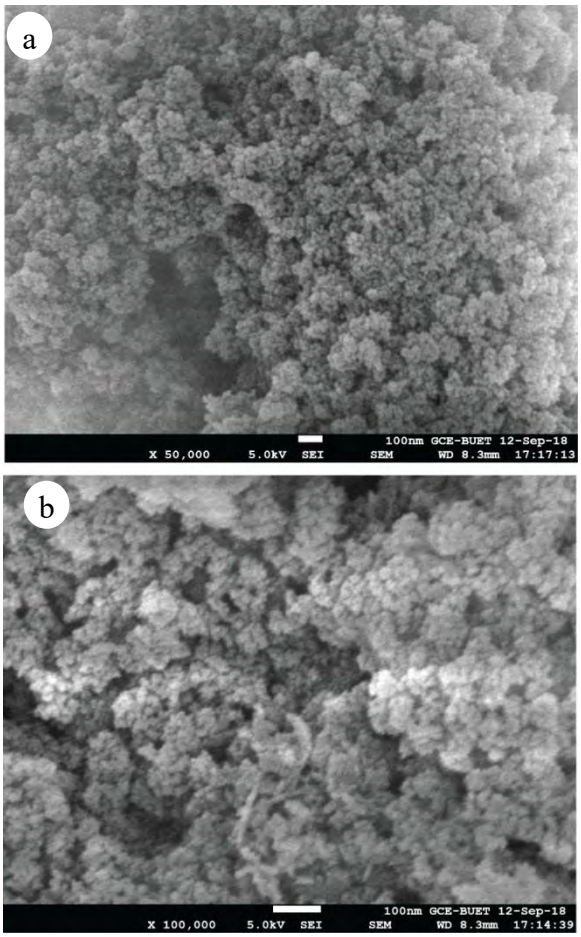

Figure 3.5 SEM images of MT composite (a) resolution x50000 (b) resolution x100000.

3.4 Energy dispersive x-ray (EDX) spectral analysis

Elemental analyses of the MT, MGOT and MTGOT nanocomposite have been performed by Energy Dispersive X-ray (EDX) method. The EDX patterns are presented in Fig. 3.7. The peaks observed at 0.277, 0.525, and 6.398 keV, for K lines of C, O, and Fe respectively. Fig. 3.5(b) and 3.5(c) exhibits that the peaks appear at 0.277, 0.525, 6.398, 1.739 and 0.392 keV for K cell of C, O, Fe and Si and N. EDX indicates the presence of C, N, O, Si and Fe on MGOT composite and MTGOT.

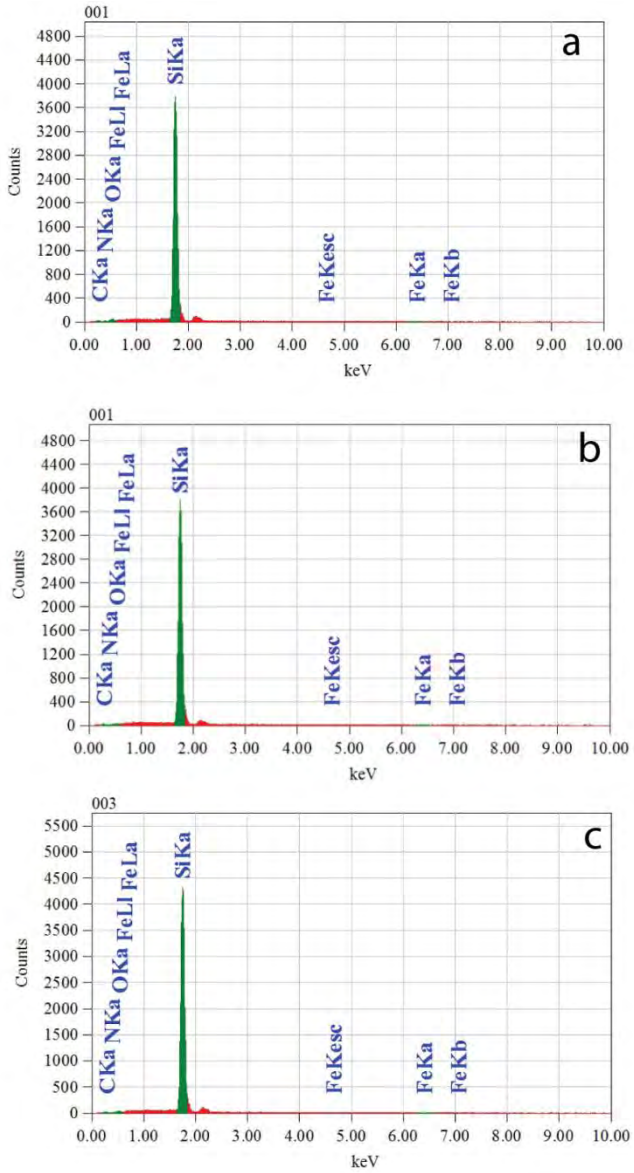

Figure 3.6 EDX spectra of (a) MT and (b) MTGO (c) MTGOT.

3.5 X-ray photoelectron spectroscopy (XPS) analysis.

3.5.1 XPS survey spectra analysis

XPS analysis revealed the elemental surface composition of the samples, including Fe, Si, O, N, and C, as summarized in Table 3.1. The XPS survey spectra (Fig.3.7) was employed to examine the composition of as prepared MGOT and MTGOT composite.

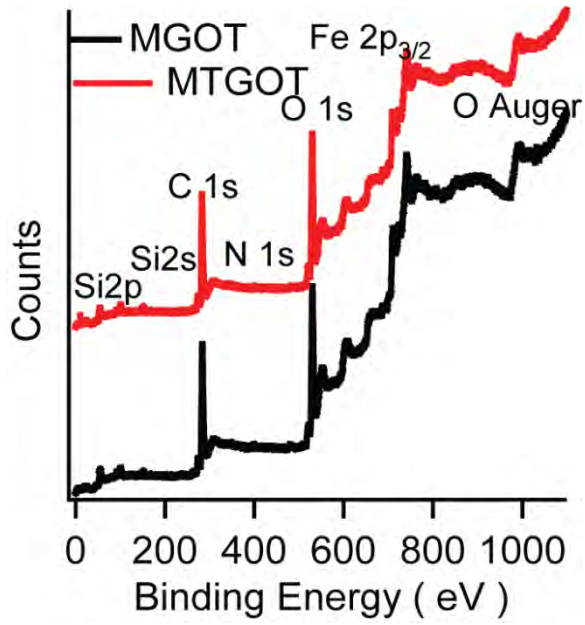

Figure 3.7. XPS survey spectra of MGOT and MTGOT nanocomposite.

It is clear that elements C, O, N and Si appear on the surface of MGO composite and C, O, N, Si and Fe in MTGOT composite. The XPS survey spectra (Fig.3.7.) was employed to examine the composition of as prepared MGOT and MTGOT composite.

Table 3.1 Chemical composition data of MGOT and MTGOT.

Compound	Fe (%)	Si (%)	C (%)	N (%)	O (%)
MTGO	2.0	3.5	66.0	0.5	28.0
MTGOT	2.0	3.8	64.0	0.8	29.8

This analysis revealed, the present of N content in MTGOT (0.8%) is more rather than MGOT (0.5%). So, magnetic graphene oxide was modified with thymine on the its surface more in MTGOT compared to MGOT.

3.5.2 High resolution C 1s spectrum analysis

The high-resolution C 1s XPS spectrum of MTGOT and MGOT can be deconvoluted four carbon states at 284.3 eV, 284.6 eV, 286.1 eV and 288.4 eV which are attributed to C-Si, C-C/C=C, C-N and C=O, respectively. These bonds mainly come from the thymine moiety on the surface of graphene oxide.

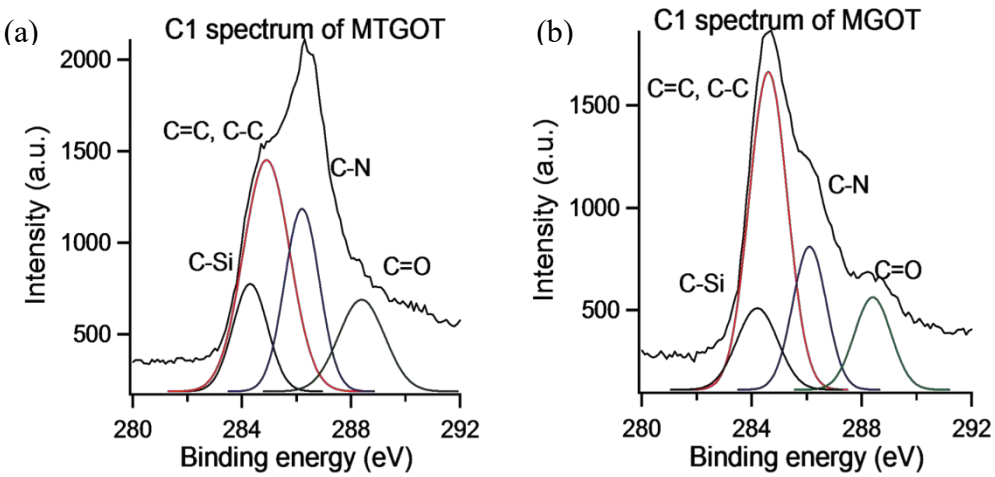

Figure: 3.8. High resolution C 1s spectrum of (a) MTGOT**,** (b) MGOT

Table: 3.2. Percentages of the bonds obtained from C 1s peak fitting for MTGOT and MGOT

Material	Bond percentages (%)			
	C-Si	C-C/C=C	C-N	C=O
MTGOT	14.9	42.8	25.3	17
MGOT	14.1	51.1	20.4	14.4

3.6 X-ray diffraction analysis (XRD)

The XRD patterns of MTGOT and MT are shown in Figure 3.9. Generally, graphite powder exhibited a typical sharp peak at 26.18°, which corresponds to an interlay distance of 0.138 nm. The graphite peak disappeared completely and shrank downward to 11.41° after chemical oxidation, which indicated that the introduction of oxygen-containing groups on the GO sheets. When the GO was reduced in high temperature a new peak appeared in 23.65°, it was revealed that the GO had been partially reduced, and the GO peak disappeared and a broad peak at around 23.18° when the GO was reacted with thymine derivative, is played in Fig. 3.9 These results implied that the GO have been attached with thymine derivative, and the GO can be reduced in high temperature.

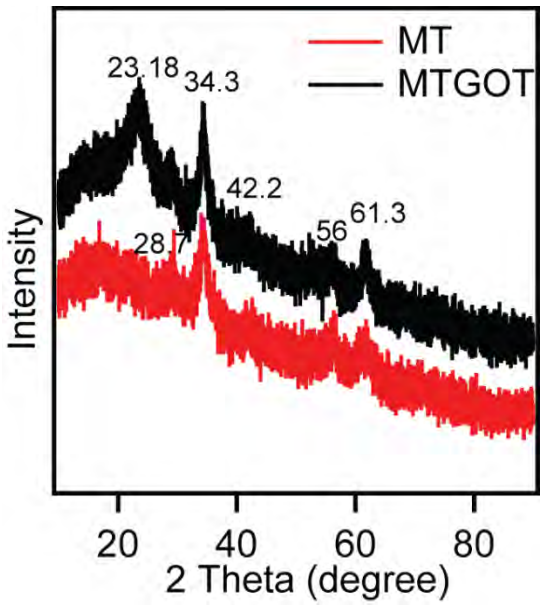

Figure 3.9 XRD spectra of MT and MTGOT composite

3.7 Magnetic property analysis

The magnetic properties of Fe_3O_4, magnetic thymine (MT), thymine immobilized magnetic graphene oxide MGOT and MTGOT were measured by VSM at room temperature (Figure 3.10)

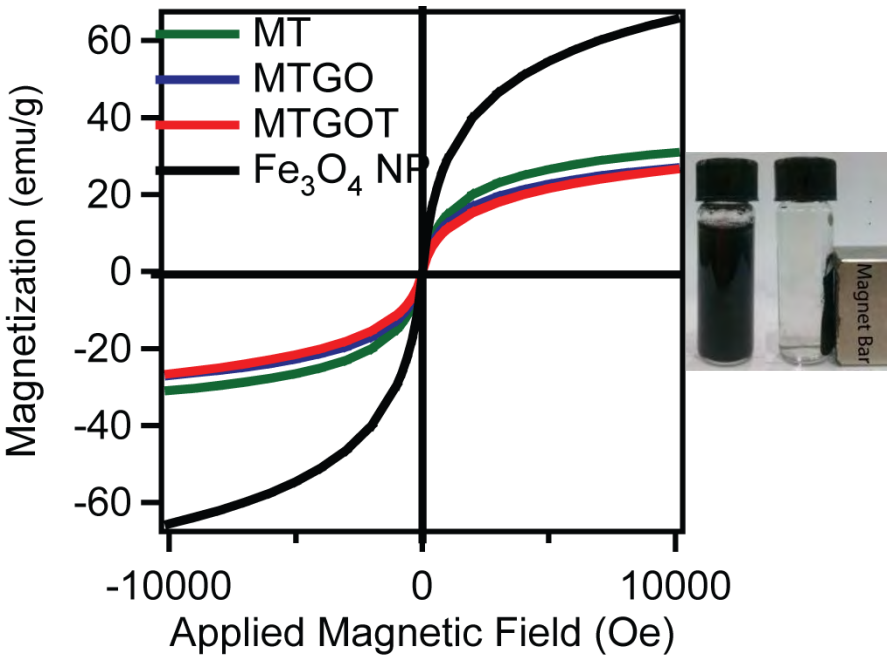

Figure 3.10 Magnetic hysteresis loops of Fe_3O_4, MT, MGOT, MTGOT (the insets show the MTGOT aqueous solution before and after magnetic separation by an external magnet).

The curves present hysteresis loop, which suggests that all of these nanoparticles exhibit ferromagnetic behavior. The magnetic saturation values are 65.5, 30.9, 26.8 and 26.7emu/g for Fe_3O_4, MT, MGOT and MTGOT. The decrease in the overall magnetization values indicates that the Fe_3O_4 surface is covered with nonmagnetic materials such as Thymine, SiO_2 and GO. Moreover, the suspensions of the MGOT and MTGOT microspheres can be rapidly concentrated on the side of the glass vial. When the magnet was removed, the nanocomposites were well dispersed again in aqueous solution after shaking, demonstrating that the nanocomposites featured with highly efficient magnetic manipulation when used as adsorbents for removal of mercury and melamine from aqueous solution under relatively low external magnetic field.

3.8 Melamine adsorption experiment

Indicators are weak acids or weak bases whose conjugate base/conjugate acid exhibits different color with change in the pH.

$$H(anion) + H_2O \longleftrightarrow Anion^- + H_3O^+$$

Several factors affect the absorbance, that is, pH, ionic strength, concentration, volume of the solution, and so forth, of which pH plays an important role in most of the analytical methods especially in case of acid-base reactions which occur in aqueous medium. In view of this, the indicator must be accordingly selected to change color when the pH of the test solution either increases or decreases. Indicator methyl red was chosen as indicators and the structure shown in Figure 3.11.

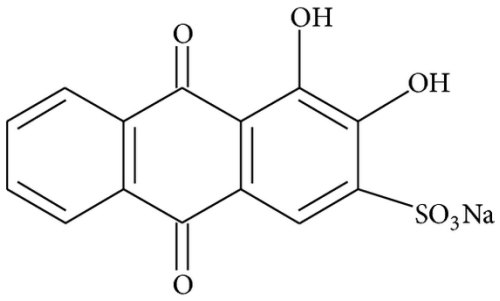

Figure 3.11. Structure of methyl red

Methyl red, $C_{15}H_{15}N_3O_2$, is an azo dye which exhibits color changes from red at pH 4.4 to yellow at pH 6.2. They have values at 2.3, 2.5, 4.95, and 5.06 [17]. The absorption maxima exhibited at 423 nm. The concentration of melamine has been examined for different mole ratios. The pH of the different concentrations of dye solutions in contact with melamine at different mole ratios leads to an increase in the pH due to the basic nature of melamine. The concentration of melamine using methyl red has been examined at different mole ratios. No visual color change observed here.

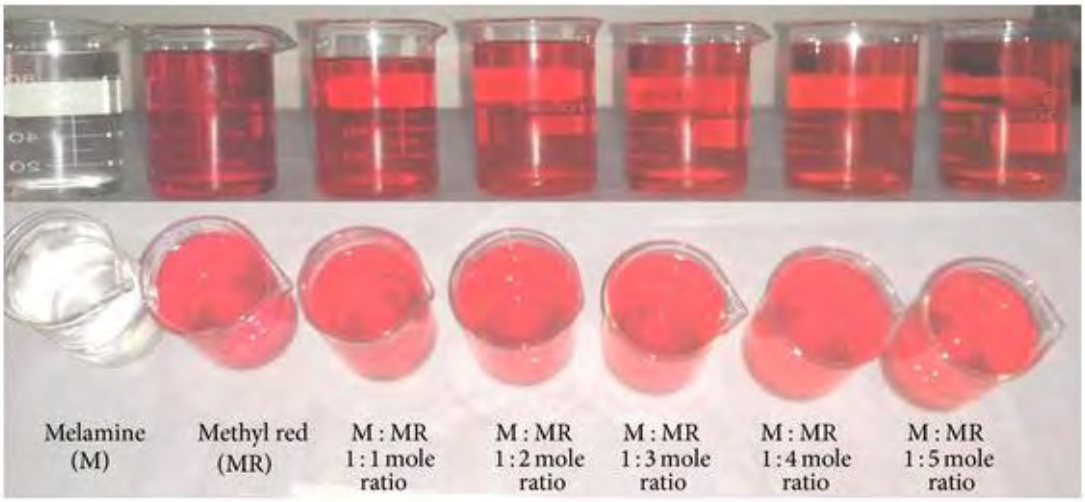

Figure 3.12. Melamine and methyl red solution mixture at different mole ratios.

Figure:3.13. illustrate the absorption spectra of melamine-dye mixture at different mole ratios with the dye concentration fixed. We observed absorption peak at 420 nm and this absorption peak decreased when methyl red and melamine are mixed in different mole ratios (melamine: methyl red ratio 1: 5).

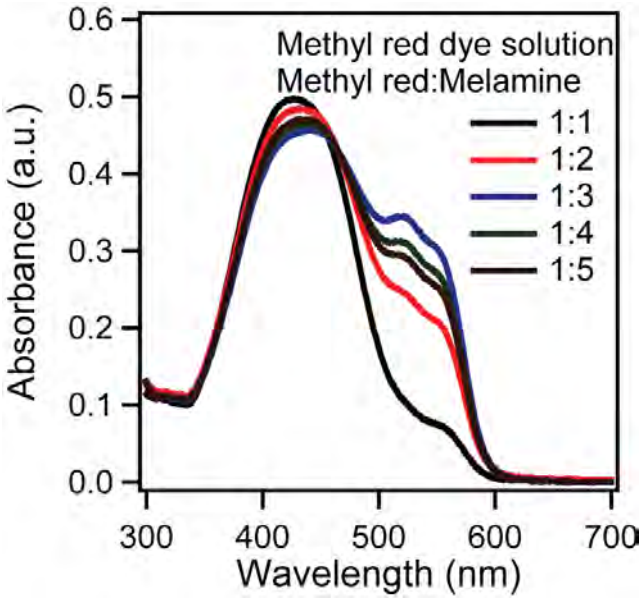

Figure 3.13. Methyl red and melamine solution with different molar ratio

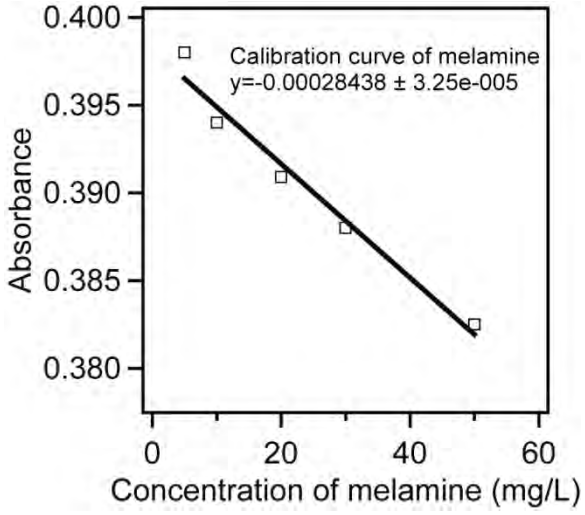

Figure 3.14. Calibration curve of melamine

Here we generated a calibration curve conc. vs absorbance of methyl red. From this calibration curve we determine the concentration of melamine after separating MTGOT and MGOT from melamine solution in different time interval. Results are shown in (Fig 3.15.)

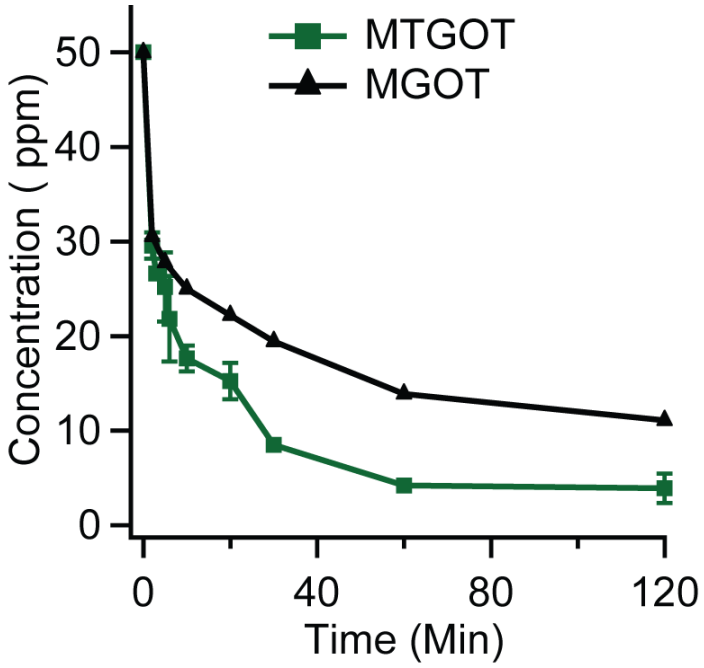

Figure 3.15. Melamine conc. Change with time

5 mg of MTGOT could remove 94% of melamine from a 50 ppm of melamine solution after 120 min, but same amount of MGOT could remove 78% because the amount of thymine moiety was present more in MTGOT rather than MGOT.

3.9 Mercury (Hg^{2+}) adsorption experiment

Batch equilibrium adsorption procedure was used to study the Hg^{2+} adsorption kinetics of MTGOT and MGOT at pH 5.0±0.2 and at room temperature using Hg^{2+} concentration of 35 mgL^{-1} and 5 mg of MGOT and MTGOT in the time range of 5 to 180 minutes. Separate the solution magnetically then the concentration of mercury was determined by CVAAS. Amount of mercury removed from the solution are shown in the figure 3.16. The removal rate (1) of mercury and the adsorption capacity (2) of MTGO and MTGOT were assessed by the following equations:

$$\text{Removal}\,(\%) = \frac{C_0 - C_e}{C_0} \times 100, \qquad (1)$$

$$q_e = \frac{(C_0 - C_e)}{m} \times V, \qquad (2)$$

Where q_e is the amount of mercury adsorbed on adsorbent at equilibrium (mgg^{-1}); C_0 and C_e are the initial and equilibrium concentrations of mercury in the solution(mgL^{-1}), respectively; $V$is the volume of solution(L); the mass of absorbent**.**

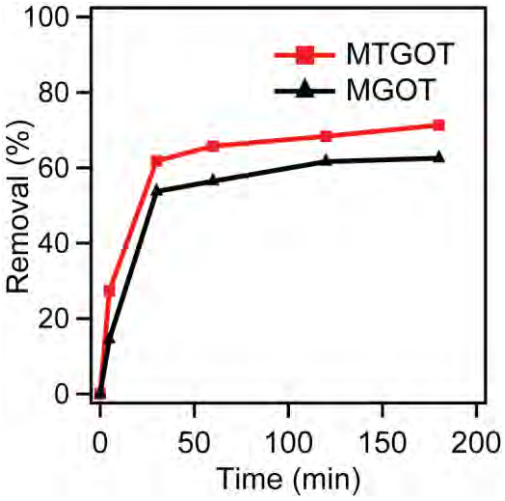

Figure 3.16 The contact time on the adsorption capability of mercury.

Figure 3.16 shows plots of the removal percentage of Hg^{2+} on MTGOT and MGOT versus contact time. The results indicated that the adsorption efficiency increased when the contact time increased from 5.0 to 30 min, and no significant change is observed from 40 to 60 min. As shown, mercury adsorption on the surface of MTGO and MGOT are a fast process and reaches the equilibrium min 40 min [18]. Here MTGOT can remove 72 % of mercury from aqueous solution but MGOT removed 63% respectively.

3.10 Conclusion

In this work, we focused on adsorptive removal of mercury (Hg^{2+}) and melamine from aqueous solutions. For this purpose, we synthesized thymine immobilized magnetic graphene oxide MTGOT and MGOT in different two procedures. Adsorption experiments of melamine was examined by UV-vis spectroscopy. On the other hand, batch equilibrium adsorption procedure was used to study the Hg^{2+} adsorption kinetics of MTGOT and MGOT at pH 5.0±0.2 and at room temperature. The XPS analysis revealed that, the amount of thymine on the surface of MGO was more in MTGOT. MTGOT showed higher adsorption efficiency compared to MGOT. MTGOT and MGOT had a Hg^{2+} adsorption capacity of 16.1 mg g^{-1} and 12.4 mg g^{-1} respectively. On the other hand, It was found that MTGOT and MGOT could remove 94.5% and 77.4%, respectively, of a 20 mL 50 ppm solution. Thus, our synthesized MTGOT and MGOT can be promising nonabsorbent for simultaneously removal of Hg^{2+} and melamine from aqueous solutions.

References

1. Y.P He, S.Q Wang, C.R Li, Y M Miao, Z Y Wu and B S Zou. “Synthesis and characterization of functionalized silica-coated Fe_3O_4 super paramagnetic nanocrystals for biological applications,” *J. Phys. D: Appl. Phys*., vol. 38, pp. 1342 2005.

2. J.S, Park, G. S. Lee, Y.J. Lee, Y.S. Park, and K. B. Yoon al."Organization of microcrystals on glass by adenine- thymine hydrogen bonding," *J. Am. Chem. Soc.*, vol.124 (45), p.p. 13366-13367, 2002.
3. M.Y, amaura, R.L. Moor "Preparation and characterization of (3-aminopropyl) triethoxysilane-coated magnetite nanoparticles*," Journal of Magnetism and Magnetic Materials*, vol. 279 (.2-3), pp.210–217 2004.
4. A. Z. M. Badruddoza, M. T. Rahman, S. Ghosh et al., "βcyclodextrin conjugated magnetic, fluorescent silica core-shell nanoparticles for biomedical applications," *Carbohydrate Polymers.*, vol.95 (1), pp.449–457, 2013.
5. Y. B. Zeng, Y. Zhou, L. Kong, T. Zhou, and G. Shi, "A novel composite of SiO_2-coated graphene oxide and molecularly imprinted polymers for electrochemical sensing dopamine," *Bio sensors and Bioelectronics.*, vol.45, (1), pp.25–33, 2013.
6. H. Zhang, X. Zhong., J.J. Xu., H. Y. Chen., "Fe_3O_4/Polypyrrole/Au nanocomposites with core/shell/shell structure: synthesis, characterization, and their electrochemical properties'', *Langmuir*, vol. 24, pp. 13748-13752, 2008.
7. R. J. J. Jansen., H. Van Bekkum., "XPS of nitrogen-containing functional groups on activated carbon'', *Carbon*, vol. 33, pp. 1021–1027, 1995.
8. S. Chu, Wang, Y.; Guo, Y.; Zhou, P.; Yu, H.; Luo, L. L.; Kong, F.; Zou, Z. G. J. *Mater. Chem*., Vol. 22, p.p. 15519−15521, 2012.
9. S.Yang., D. P., Zhang Min, X. Zhonglei, and C. Lihong. "Preparation of Graphene Oxide Decorated Fe3O4@SiO2 Nanocomposites with Superior Adsorption Capacity and SERS Detection for Organic Dyes", *Journal of Nanomaterials.,* vol. 2015, p.p. 8, 2015.
10. C. H. Chung, J. H. Kim, and B. H. Chung, "Detection of UV-induced mutagenic Thymine imer Using Graphene Oxide," *Anal. Chem.*, vol. *86* (23), pp 11586–11591, 2014.

11. Y. B.; Sun, C. C.; Ding, W. C.; Cheng, X. K. Wang, "Simultaneous adsorption and reduction of U(VI) on reduced graphene oxide-supported nanoscale zerovalent iron", *J. Hazard. Mater*., vol.280, p.p. 399, 2014.
12. M. Fang., V. Strom., R. T. Olsson., L. Belova., K. V. Rao., "Particle size and magnetic properties dependence on growth temperature for rapid mixed co-precipitated magnetite nanoparticles'', Nanotech., vol. 23, pp. 145601, 2012.
13. X.; Feng, G. E. Fryxell, L. Q. Wang, A. Y. Kim, J.Liu, K. M. Kemner, "Functionalized Monolayers on Ordered Mesoporous Supports," *Science*, vol. 276, p.p 923−926, 1997.
14. Z. H. Qin, H. W. Zhao, C. Z. Huang, and L. P. Wu, "Visual detection of melamine in raw milk by label-free silver nanoparticles," *Chemistry Letters*, vol. 38, p.p. 470–471, 2009.
15. L. J. Mauer, A. A. Chernyshova, A. Hiatt, A. Deering, and R. Davis, "Melamine detection in infant formula powder using near- and mid-infrared spectroscopy," *Journal of Agricultural and Food Chemistry.*, Vol. 57 (10), p.p. 3974–3980 (2009).
16. R.T. Ashandra and K. D. Sahally. "Visual detection and determination of melamine using synthetic dyes," *Journal of Applied chemistry*., vol. 2014, p.p. 7, 2014.
17. D. H. Wu, Q. Zhang, X. Chu, H. B. Wang, G. L. Shen, Yu, R. Q. Ultrasensitive Electrochemical Sensor for Mercury (II) Based on Target-Induced Structure-Switching DNA. *Biosens. Bioelectron*., vol.25, p.p. 1025−1031, 2010.
18. Z. Wang, D. Zhang, D. A. Zhu, Sensitive and Selective "Turn on" Fluorescent Chemosensor for Hg (II) Ion Based on a New Pyrene Thymine Dyad. *Anal. Chim. Acta*., vol. 549, p.p. 10−1, 2005.